ALMA MATER STUDIORUM
UNIVERSITÀ DI BOLOGNA

DEPARTMENT OF PHYSICS AND ASTRONOMY "A. RIGHI"

SECOND CYCLE DEGREE
PHYSICS

Integral Reduction In Loop-by-Loop Baikov Representation

Supervisor
Prof. Tiziano Peraro

Co-supervisor
Dr. Dhimiter Canko

Defended by
Pietro Vallicelli

Graduation Session / 03/ 2026

Academic Year 2024/2025

Abstract

Feynman loop integrals represent a fundamental topic in the study of scattering amplitudes within quantum field theory. In this dissertation we present an approach for the analysis of multi-loop Feynman integrals properties, employing syzygy equations within the loop-by-loop Baikov representation. By identifying propagators as integration variables and performing the parametrization iteratively, this framework generates a more compact system of Integration-by-Parts identities, an essential tool to perform the so called integral reduction of an integral family. Furthermore, our analysis includes the derivation of the differential equations for both families using polynomial decomposition techniques, which further optimize the reduction process. The results are successfully validated by applying our algorithm to two two-loop cases: the massless box-triangle and double-box families.

Contents

Chapter 1

Introduction

Scattering amplitudes are the central objects of study in quantum field theory, representing a fundamental connection between theoretical frameworks and experimental observations. In the context of modern particle physics, particularly for experiments at the Large Hadron Collider (LHC), these amplitudes are essential for translating the underlying Lagrangian of the Standard Model into observable quantities, such as cross-sections and decay rates.

To achieve the level of precision required by current experimental data–often reaching the per-cent level for many observables–theoretical predictions must be computed beyond the tree-level approximation. This necessitates the evaluation of higher-order terms in the perturbative expansion, which are represented by Feynman loop integrals. As the number of loops and external legs increases, these integrals become difficult to evaluate, forming a primary computational bottleneck in high-energy physics.

Traditionally, Feynman integrals are formulated in momentum space. While this representation is useful for understanding the analytic structure of Green functions, it is often cumbersome for direct multi-loop evaluations. This has led to the development of alternative parametrizations, such as the Schwinger representation [1–3] and the Lee-Pomeransky representation [4]. A further shift in perspective is provided by the Baikov representation [5–7]. In particular, the Baikov parametrization—and its loop-by-loop variant[8]—is specifically designed to exploit the algebraic properties of the integrals. In this framework, the integration variables are identified with the propagators themselves.

Indeed, Feynman integrals within the same family are not independent; they are related by a vast system of linear relations, most notably Integration-by-Parts (IBP) identities [9, 10]. In particular, IBPs are highly employed in the so called integral reduction, whose objective is to identify a set of independent integrals, known as master integrals, through which any other integral in the family can be expressed.

However, as the complexity of the process grows, the system of IBP identities leads to significant algebraic challenges. To optimize this process, modern techniques employ syzygy equations within the Baikov framework [11–14]. This synergy allows for the gen-

eration of IBP identities that are more efficient, specifically by avoiding the appearance of higher powers in the propagators —a major source of complexity in standard reduction schemes. The latter is particularly important for multi-scale, multi-loop computations, where the system of generated IBPs grows rapidly. In this context, reducing both the scattering amplitude and the derivatives of the master integrals (needed for constructing differential equations [15, 16]) becomes highly challenging, if not impossible.

The primary objective of this work is to present and implement an efficient framework for the integral reduction of multi-loop families. Specifically, we aim to:

- Develop a reduction scheme within the loop-by-loop Baikov representation, integrated with syzygy techniques, to highlight the advantages of this approach over traditional methods.
- Extend the analysis to the derivation of the differential equations obeyed by the master integrals, employing a polynomial decomposition approach.
- Validate the proposed methodology through concrete two-loop examples, such as the massless box-triangle and double-box families, comparing the correctness of the results against established Laporta-based algorithms.

This thesis is organized as follows. In Chapter 2 we review fundamental concepts to the study of Feynman loop integrals such as IBP relations and their role in the integral reduction to find a set of master integrals. Moreover we review the method of differential equations to find the master integrals and analyze their properties. In Chapter 3 we review the Baikov representation and its loop-by-loop variant, highlighting their advantages and drawbacks, providing examples for two multi-loop cases: the massless box-triangle and the massless double-box families. Furthermore, we review the theory of syzygy equations and how it is employed in the construction of IBPs in the standard Baikov representation. In Chapter 4 we present the algorithm built to perform a proper integral reduction in the loop-by-loop Baikov framework, using syzygy equations. We apply our algorithm to the box-triangle and double-box families. In Chapter 5 we broaden our analysis to the study of the system of differential equations obeyed by the master integrals obtained from the reduction of the box-traingle and double-box families. In order to do so, we employ a polynomial decomposition method. Finally, Chapter 6 we summarize our findings.

The thesis is complemented by three appendices: Appendix A provides an additional example of differential equations for the one-loop box family; Appendix B contains a detailed derivation of the various forms of the Baikov representation; and Appendix C describes the numerical methods implemented in the `FiniteFlow` framework [17], which served as the computational backbone for all the calculations presented in this work.

Chapter 2

Loop Integrals and Feynman Representation

In this chapter we review Feynman integrals and their fundamental properties, with particular emphasis on their singularity structure and the role of IBP identities [9, 10]. Furthermore, we introduce the essential tools for their evaluation, ranging from the Feynman parametric representation to the systematic organization of integrals into families. Finally, we discuss the reduction to a basis of master integrals [18] and the derivation of the associated system of differential equations [15, 16], which constitute the backbone of modern multi-loop calculations. The discussion in this chapter follows the treatment provided in [19], which serves as our primary reference. Representative examples are included for each of the introduced concepts.

2.1 Introduction to Feynman Integrals

Feynman integrals (FIs) constitute the fundamental framework for performing perturbative predictions in quantum field theory. Beyond their historical role in particle physics, they have emerged as indispensable tools for computing physical observables across diverse research areas, including general relativity and the study of gravitational waves. We can associate a *Feynman graph* to a FI (and vice-versa), defined as a directed graph with external half-edges (*external legs*) and internal edges (*propagators*), connected via points named *vertices* respecting momentum conservation.

A graph can have independent cycles inside, each of them called *loop*, with an associated arbitrary loop momentum. Moreover, external legs' momenta are linear combinations of the momenta associated to the external particles of the process, while the propagators are defined by a mass and a momentum which is a combination of both the loop and external momenta.

Divergences naturally arise in FIs as a consequence of the integration over loop mo-

menta. Given that physical observables must be finite, these singularities are handled through a regularization procedure, ensuring they cancel at later stages of the calculation or through renormalization. The most widely adopted method is dimensional regularization, where the spacetime dimension is analytically continued from 4 to $D = 4 - 2\epsilon$. Within this framework, ultraviolet and infrared singularities manifest as Laurent poles in the regulator ϵ.

Furthermore, the analytic study of the integrands allows us to characterize the functional space to which loop integrals belong. While many integrals can be expressed in terms of well known functions such as logarithms and multiple polylogarithms, more complicated structures often are involved, e.g. elliptic integrals. Further details and a more in-depth analysis are available in standard literature [20], [21].

2.2 Notation and Conventions

We start our analysis by setting the stage for (one-loop) Feynman integral computations, defining our notation and conventions. First of all, we always work in Minkowski flat space-time

$$\eta_{\mu\nu} = \text{diag}(+1, -1, -1, -1). \tag{2.1}$$

Considering the D-dimensional extension, we get

$$\eta_{\mu\nu} = \text{diag}\big(+1, \underbrace{-1, -1, \ldots, -1}_{D-1}\big). \tag{2.2}$$

The integrands of FIs are built through D-dimensional propagators which, for a particle of mass m and momentum p, read as

$$\frac{i}{p^2 - m^2 + i\epsilon}, \tag{2.3}$$

where $\epsilon \to 0^+$ is the well known Feynman prescription i.e. a small, positive imaginary part that moves the poles of the propagator off the real axis. Here we used a compact notation for the squared momentum $p^2 \equiv \eta_{\mu\nu} p^\mu p^\nu = p_\mu p^\mu$. We use the convention that external momenta are labeled p_i, with $i = 1, 2, \ldots, E$ and loop momenta are denoted k_j, with $j = 1, 2, \ldots, L$, where E is the number of external legs in the graph and L is the number of loops.

In order to explain how FIs look at loop level, we present the following example:

$$I_a = \int \frac{\mathrm{d}^D k}{i\pi^{D/2}} \frac{1}{(k^2 - m^2 - i\epsilon)^a} = \int \frac{\mathrm{d}^D \mathbf{k}}{i\pi^{D/2}} \int \frac{\mathrm{d}\, k_0}{(k_0^2 - \mathbf{k}^2 - m^2 - i\epsilon)^a}, \tag{2.4}$$

where $k = (k_0, \mathbf{k})$ and a is an arbitrary integer. We will see later that there are specific values for D and a that guarantee the convergence of the integral. Firstly, we integrate over k_0, performing a *Wick rotation*. In fact, we notice that we encounter two poles in the k_0 complex plane:

$$k_0^{\pm} = \pm\sqrt{\mathbf{k}^2 + m^2} \mp i0^-. \tag{2.5}$$

We can rotate the integration contour without crossing the poles, so that the new contour is parallel to the imaginary axis:

$$k_0 = ik_{0,E}. \tag{2.6}$$

We can rewrite eq. (2.4) as follows:

$$I_{a,E} = \frac{1}{(-1)^a} \int \frac{\mathrm{d}^D k_E}{\pi^{D/2}} \frac{1}{(k_E^2 + m^2 - i\epsilon)^a}, \tag{2.7}$$

in which we defined a Euclidean D-dimensional vector $k_E = (k_{0,E}, \mathbf{k})$. Now, in order to solve eq. (2.7) we use *Schwinger parametrisation*

$$\frac{1}{x^a} = \frac{1}{\Gamma(a)} \int_0^\infty \mathrm{d}\,\alpha \alpha^{a-1} e^{-\alpha x}. \tag{2.8}$$

In our case, $x = (k_E^2 + m^2)$. We can use Gaussian integration to compute

$$\int d^D k_E e^{-\alpha k_E^2} = \left(\frac{\pi}{\alpha}\right)^{D/2}. \tag{2.9}$$

Last step consists in applying again Schwinger parametrisation, to get the final result

$$I_a = \frac{1}{(-1)^a} \frac{\Gamma(a - D/2)}{\Gamma(a)} \frac{1}{(m^2 - i\epsilon)^{a-D/2}}. \tag{2.10}$$

Notice that, assumed D and a to be integers, the convergence conditions are $a > 0$ and $a - D/2 > 0$. We will see in next section, the motivations and the meaning of defining non-integer D.

2.2.1 UV and IR Divergences

In quantum field theory one often has to deal with divergences. In particular, there are two cases:

- Ultraviolet (UV) divergences: they are related to renormalisation of couplings, wavefunctions and masses in quantum field theory. They can be handled via *dimensional regularisation* i.e. by setting $D = 4 - 2\epsilon$, with $\epsilon \to 0^+$.

- Infrared (IR) divergences: they arise when massless particles are involved in on-shell processes. We can have *soft* divergences (when the loop momenta are close to zero) and *collinear* divergences (when a loop momentum is collinear to an external on-shell momentum). They can be treated with dimensional regularisation, but with $\epsilon \to 0^-$.

A detailed discussion of the renormalization procedure and the treatment of infrared singularities lies beyond the scope of this work. For a complete review of these topics, the reader is referred to [20], [21].

2.3 Feynman Representation

In the previous section we have seen how to compute the simplest case of Feynman integral. Now our purpose extends to the computation of more complex integrals, with arbitrary number of loops and external particles. In general, a FI depends on parameters such as external momenta p_i (which can be on-shell or not) and masses m_j. The most generic expression for an L-loop Feynman Integral, in D dimensions is

$$I(p_i; m_j; D) = \int \mathrm{d}^D k_1 \dots \mathrm{d}^D k_L I(p_i; k_j; m_k). \tag{2.11}$$

Let us analyze now an explicit example, consider a generic n-point massive one loop scalar FI:

$$I^{1-loop}_{a_1,\dots,a_n} = \int \frac{\mathrm{d}^D k}{i\pi^{D/2}} \frac{1}{D_1^{a_1} \dots D_n^{a_n}}, \tag{2.12}$$

where the propagators are defined as

$$D_i = q_i^2 - m_i^2, \tag{2.13}$$

and the momenta q_i are linear combination of the loop momentum k and the external momenta p_i.

In order to evaluate $I^{1-loop}_{a_1,\dots,a_n}$ it is convenient to introduce a set of integration variables, the so called *Feynman parameters* α_i. Firstly, we consider the following identity

$$\frac{1}{\prod_{i=1}^n D_i^{a_i}} = \frac{(a-1)!}{(a_1-1)!\dots(a_n-1)!} \int_0^\infty \frac{\mathrm{d}\,\alpha_1\,\mathrm{d}\,\alpha_2 \dots \mathrm{d}\,\alpha_n}{GL(1)} \frac{\alpha_1^{a_1-1}\alpha_2^{a_2-1}\dots\alpha_n^{a_n-1}}{(\alpha_1 D_1 + \alpha_2 D_2 + \dots + \alpha_n D_n)^a}, \tag{2.14}$$

with $a = \sum_{i=1}^n a_i$. The term $GL(1)$ signals that the r.h.s. is invariant under arbitrary rescalings of $\alpha_1, \dots, \alpha_n$ (i.e. general linear transformations). For example, if $n = 2$, one can fix $\alpha_1 + \alpha_2 = 1$ so that the $GL(1)$ term has the effect of inserting a Dirac δ-function

of the form $\delta(\alpha_1+\alpha_2-1)$ in the integrand. The proof of the formula above can be found in standard literature such as [20].

Finally, using the properties of the Euler Gamma function we can generalize eq. (2.14) to

$$\frac{1}{\prod_{i=1}^{n} D_i^{a_i}} = \frac{\Gamma(a)}{\prod_{i=1}^{n}\Gamma(a_i)} \int_0^\infty \frac{\mathrm{d}\,\alpha_1\,\mathrm{d}\,\alpha_2\ldots\mathrm{d}\,\alpha_n}{GL(1)} \frac{\alpha_1^{a_1-1}\alpha_2^{a_2-1}\ldots\alpha_n^{a_n-1}}{(\alpha_1 D_1+\alpha_2 D_2+\cdots+\alpha_n D_n)^a}, \tag{2.15}$$

Applying the identity (2.15) to the definition of $I^{1-loop}_{a_1,\ldots,a_n}$ we obtain the general formula

$$I^{1-loop}_{a_1,\ldots,a_n} = \frac{1}{(-1)^a}\frac{\Gamma(a-D/2)}{\prod_{i=1}^{n}\Gamma(a_i)} \int_0^\infty \frac{\prod_{i=1}^{n}\mathrm{d}\,\alpha_i\alpha_i^{a_i-1}}{GL(1)} \frac{U^{a-D}}{(V+U\sum_{i=1}^{n} m_i^2\alpha_i - i0^+)^{a-D/2}}, \tag{2.16}$$

In particular,

$$\begin{aligned} U &= \sum_{i=1}^{n}\alpha_i, \\ V &= \sum_{i<j}\alpha_i\alpha_j(-x_{ij}^2), \end{aligned} \tag{2.17}$$

where $x_{ij}\equiv x_i - x_j$ are related to the dual coordinates x_i defined as

$$\begin{aligned} k &= x_0 - x_1, \\ p_i &= x_{i+1} - x_i. \end{aligned} \tag{2.18}$$

U and V are called *Symanzik polinomials*, for more details about the structure and the definition of these polynomials see [22]. Furthermore, one may fix the $GL(1)$ freedom in many ways, for example by setting $U=1$ i.e. $\sum_{i=1}^{n}\alpha_i = 1$. Before presenting a one-loop example, let us mention the generalisation of the master formula (2.16) for L loops.

In particular, considering a generic n-point massive L-loops scalar FI:

$$I^{L-loops}_{a_1,\ldots,a_n} = \int \prod_{j=1}^{L} \frac{\mathrm{d}^D k_j}{i\pi^{D/2}} \left(\frac{1}{D_1^{a_1} D_2^{a_2}\ldots D_n^{a_n}}\right). \tag{2.19}$$

$$I^{L-loops}_{a_1,\ldots,a_n} = \frac{1}{(-1)^a}\frac{\Gamma(a-LD/2)}{\prod_{i=1}^{n}\Gamma(a_i)} \int_0^\infty \frac{\prod_{i=1}^{n}\mathrm{d}\,\alpha_i\alpha_i^{a_i-1}}{GL(1)} \frac{U^{a-LD}}{(V+U\sum_{i=1}^{n} m_i^2\alpha_i - i0^+)^{a-LD/2}}, \tag{2.20}$$

where U and V have the same definition of the 1-loop case.

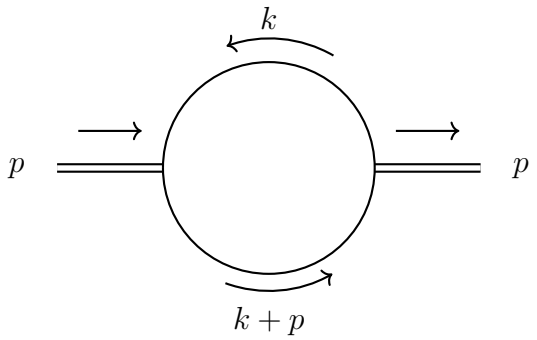

Figure 2.1: Bubble diagram with double external lines representing massive particles.

2.3.1 Example: The Massless Bubble Integral

In this section we present an example of the application of the general formula (2.16) to a simple one loop scalar case: the massless bubble integral, shown in fig. 2.1.

We aim to write down the Feynman parametrisation and evaluate the bubble diagram in fig. 2.1. Firstly, its corresponding Feynman integral is

$$I_{bubble}(a_1, a_2; D) = \int \frac{\mathrm{d}^D k}{i\pi^{D/2}} \frac{1}{(k^2 - i0^+)^{a_1}((k+p)^2 - i0^+)^{a_2}}. \tag{2.21}$$

Now, applying the identity (2.15) with $n = 2$, $D_1 \equiv k^2$, $D_2 \equiv (k+p)^2$, we obtain

$$I_{bubble} = \frac{\Gamma(a_1 + a_2)}{\Gamma(a_1)\Gamma(a_2)} \int \frac{\mathrm{d}\,\alpha_1\,\mathrm{d}\,\alpha_2}{GL(1)} \int \frac{\mathrm{d}^D k}{i\pi^{D/2}} \frac{\alpha_1^{a_1-1}\alpha_2^{a_2-1}}{[\alpha_1 k^2 + \alpha_2(k+p)^2]^{a_1+a_2}}. \tag{2.22}$$

If we define $M^2 \equiv k^2 + \frac{2\alpha_2}{\alpha_1+\alpha_2} k \cdot p + \frac{\alpha_2}{\alpha_1+\alpha_2} p^2$, we can rewrite

$$I_{bubble} = \frac{\Gamma(a_1 + a_2)}{\Gamma(a_1)\Gamma(a_2)} \int \frac{\mathrm{d}\,\alpha_1\,\mathrm{d}\,\alpha_2}{GL(1)} \int \frac{\mathrm{d}^D k}{i\pi^{D/2}} \frac{\alpha_1^{a_1-1}\alpha_2^{a_2-1}(\alpha_1+\alpha_2)^{-a_1-a_2}}{(M^2)^{a_1+a_2}}. \tag{2.23}$$

We can complete squares in the M^2 definition and define a shifted momentum $\tilde{k}$

$$\tilde{k} \equiv k + \frac{\alpha_2}{\alpha_1 + \alpha_2} p, \tag{2.24}$$

yielding

$$I_{bubble} = \frac{\Gamma(a_1 + a_2)}{\Gamma(a_1)\Gamma(a_2)} \int \frac{\mathrm{d}\,\alpha_1\,\mathrm{d}\,\alpha_2 \alpha_1^{a_1-1}\alpha_2^{a_2-1}(\alpha_1+\alpha_2)^{-a_1-a_2}}{GL(1)} \int \frac{\mathrm{d}^D \tilde{k}}{i\pi^{D/2}} \frac{1}{[\tilde{k}^2 + \frac{\alpha_1\alpha_2 p^2}{(\alpha_1+\alpha_2)^2}]^{a_1+a_2}}. \tag{2.25}$$

We can use eq. (2.10) to integrate over $\tilde{k}$ and obtain

$$I_{bubble} = \frac{\Gamma(a_1 + a_2 - D/2)}{\Gamma(a_1)\Gamma(a_2)} \int \frac{\mathrm{d}\,\alpha_1\,\mathrm{d}\,\alpha_2 \alpha_1^{a_1-1}\alpha_2^{a_2-1}}{GL(1)} \frac{(\alpha_1+\alpha_2)^{a_1+a_2-D}}{(-\alpha_1\alpha_2 p^2)^{a_1+a_2-D/2}}, \tag{2.26}$$

from which we can read off

$$U = \alpha_1 + \alpha_2, \quad V = -\alpha_1\alpha_2 p^2. \tag{2.27}$$

Now that we have wrote the Feynman parametrisation for the bubble integral, we are ready to evaluate it. Next step consists in employing the $GL(1)$ invariance to insert in the integrand a Dirac δ-function of the form $\delta(\alpha_1 + \alpha_2 - 1)$, so that

$$I_{bubble} = (-p^2)^{-a_1-a_2+D/2} \frac{\Gamma(a_1 + a_2 - D/2)}{\Gamma(a_1)\Gamma(a_2)} \int_0^1 \mathrm{d}\,\alpha_1 \alpha_1^{D/2-a_2-1}(1-\alpha_1)^{D/2-a_1-1}. \tag{2.28}$$

Using the Euler Beta function definition we get the final result

$$I_{\text{bubble}}(a_1, a_2; D) = \frac{\Gamma(a_1 + a_2 - D/2)\,\Gamma(D/2 - a_1)\,\Gamma(D/2 - a_2)}{(-1)^{a_1+a_2}\Gamma(a_1)\,\Gamma(a_2)\,\Gamma(D - a_1 - a_2)} (-p^2)^{D/2-a_1-a_2}. \tag{2.29}$$

2.4 Integral Families, IBPs and Master Integrals

In this section we discuss how to group FIs in sets, according to their propagator structure and kinematics, defined as *integral families*. In order to study their properties we will analyze how to write IBPs in order to find the *master integrals* (MIs) of a given family.

Firstly, we define the set of integrals in eq. (2.19) as an *integral family*. In particular, $a_1, ...a_n$ are arbitrary integers, thus this definition describes an infinite number of FIs with different values of a_i. Let us recall that, when the integer $a_i > 0$, D_i represents a usual propagator; conversely, when $a_i \leq 0$, D_i moves to the numerator, representing a propagator-like object called *irreducible scalar product* (ISP).

Now, an integral family contains infinitely many elements, which are a linear combination of a finite subset $\{G_k\}$ of objects called *master integrals*. In other words, we can define a finite-dimensional basis in this space and its elements are the MIs. Thus we can write $I_j = \sum_j c_{jk} G_k$, with $\{G_k\} \subset \{I_k\}$.

For example, massive bubble integrals of mass m, loop momentum k, external momentum p and arbitrary integer powers (a_1, a_2) in the propagators, belong to the family

$$I_{a_1,a_2} = \int \frac{\mathrm{d}^D k}{i\pi^{D/2}} \frac{1}{[k^2 - m^2]^{a_1}[(k+p)^2 - m^2]^{a_2}}. \tag{2.30}$$

In order to find the MIs, the most useful tools are IBPs [9, 10]. They arise from the fact that, in dimensional regularisation, total derivatives vanish. We can write IBPs for integrals within a family

$$\int \prod_{j=1}^{L} \frac{\mathrm{d}^D k_j}{i\pi^{D/2}} \frac{\partial}{\partial k_{j\mu}} \frac{v^\mu}{D_1^{a_1} \dots D_n^{a_n}} = 0, \tag{2.31}$$

where $v^\mu = \sum_j (\alpha_{ij} p_j^\mu + \beta_{ij} k_j^\mu)$ and $\{k_{j\mu}\}$, $\{a_i\}$ are arbitrarily chosen.

2.4.1 Example: The Massive Bubble Family

Let us review explicitly the massive bubble integral family example (2.30), following the treatment presented in [23]. The IBPs are obtained by

$$\int \prod_{j=1}^{L} \frac{\mathrm{d}^D k_j}{i\pi^{D/2}} \frac{\partial}{\partial k_\mu} \left\{ v^\mu \frac{1}{[k^2 - m^2]^{a_1} [(k+p)^2 - m^2]^{a_2}} \right\} = 0. \tag{2.32}$$

If we choose $v^\mu = k^\mu$ and we set $p^2 \equiv s$, we get the IBP relation

$$(D - 2a_1 - a_2) I_{a_1,a_2} - 2m^2 a_1 I_{a_1+1,a_2} + (s - 2m^2) a_2 I_{a_1,a_2+1} - a_2 I_{a_1-1,a_2+1} = 0. \tag{2.33}$$

Whereas, choosing $v^\mu = p^\mu$, we obtain the identity

$$(a_1 - a_2) I_{a_1,a_2} - a_1 I_{a_1+1,a_2-1} + a_2 I_{a_1-1,a_2+1} + s a_1 I_{a_1+1,a_2} - s a_2 I_{a_1,a_2+1} = 0. \tag{2.34}$$

Eqs. (2.33), (2.34) are IBPs for arbitrary values of the propagators powers $\{a_j\}$; these kind of identities are called *template equations*. We can find an additional identity obeyed by this family, which arises from the following symmetry relation. In fact, if we perform a shift $k^\mu \to \tilde{k}^\mu = k^\mu + p^\mu$, we obtain $D_1 \leftrightarrow D_2$, i.e.

$$I_{a_1,a_2} = I_{a_2,a_1}. \tag{2.35}$$

Notice that this result could have been computed in the same way, if we chose $v^\mu \equiv k^\mu + p^\mu$ in eq. (2.32). As we stated earlier, we recall that IBPs can be used to reduce the integrals of a given family to a finite number of MIs, this process is called *integral reduction*. The general strategy to perform the reduction consists in two combined steps:

- Simplify the template equations, keeping $\{a_j\}$ symbolic.
- Replace a_j with integer values to get explicit equations.

The most famous technique for performing an integral reduction is *Laporta algorithm* [18]. Within this algorithm, the integrals are assigned a weight according to their complexity. The weight choice is completely arbitrary, for example one can assign the lower weight to integrals that have fewer propagators. Then, for the provided integrals, IBPs are generated and solved using Gaussian elimination, expressing higher-weight integrals in terms of lower-weight ones.

The MIs are chosen to be those integrals that remain undetermined from this protocol. It is important to highlight that the choice of MIs is not unique, as one can provide a lower index for specific integrals in this procedure, and a convenient choice may help in the reduction. There exist several publicly-available packages that implement Laporta's algorithm, such as `Blade` [24], `AIR` [25], `FIRE` [26], `KIRA`[27], `REDUZE` [28], `Azurite` [29], `NeatIBP` [13] etc.

Going back to our example, we can perform the calculation explicitly. First of all, in order to better organise the reduction, we divide the family into *sectors*, defined as

$$S[I_{a_1,a_2,\ldots,a_n}] = S[a_1,\ldots,a_n] = \left\{\theta\left(a_1-\frac{1}{2}\right),\theta\left(a_2-\frac{1}{2}\right),\ldots,\theta\left(a_n-\frac{1}{2}\right)\right\}, \tag{2.36}$$

where $\theta(x)$ is the Heaviside function. For example, $S[1,2] = S[1,1] = \{1,1\}$ and $S[0,2] = S[-1,1] = \{0,1\}$. As stated before, we proceed from sectors with fewer denominators to higher.

- $\{0,0\} \leftrightarrow a_1 \leq 0, a_2 \leq 0$. For this sector we have $I_{a_1,a_2} = 0$, since scaleless integrals vanish in dimensional regularisation.

- $\{1,0\} \leftrightarrow a_1 > 0, a_2 \leq 0$. For this sector, we substitute in eq. (2.33) suitable values for (a_1,a_2) such as $(a_1,a_2) = (1,0)$, obtaining

$$I_{2,0} = \frac{D-2}{2m^2} I_{1,0}. \tag{2.37}$$

  If we substitute $(a_1,a_2) = (1,0)$ in eq. (2.34) we get

$$I_{2,-1} = I_{1,0} + sI_{2,0} = \left(1 + s\frac{D-2}{2m^2}\right) I_{1,0}. \tag{2.38}$$

  Moreover, using $(a_1,a_2) = (1,-1)$ in both template equations, we find

$$\begin{aligned} I_{1,-1} &= sI_{1,0}, \\ I_{2,-2} &= s\left(4 + \frac{D-2}{2m^2}\right) I_{1,0}. \end{aligned} \tag{2.39}$$

- $\{0,1\} \leftrightarrow \{1,0\}$ due to the symmetry relation (2.35).

- $\{1,1\} \leftrightarrow a_1 > 0, a_2 > 0$. We choose $(a_1, a_2) = (1,1)$ in eq. (2.33), obtaining

$$I_{2,1} = -\frac{D-2}{2m^2(4m^2-s)}\, I_{1,0} + \frac{D-3}{4m^2-s}\, I_{1,1} \tag{2.40}$$

In this case, we have chosen the MIs to be $\{\tilde{G}_j\} = \{I_{1,0}, I_{1,1}\}$. Notice that we could have picked any other two independent integrals to be MIs. For example, we can arbitrarily choose $\{\tilde{G}_j\} = \{I_{1,1}, I_{2,0}\}$ so that each integral of the family can be written in terms of the MIs

$$\begin{cases} I_{1,0} = \dfrac{2m^2}{D-2} I_{2,0}, \\ I_{2,-1} = \left(s + \dfrac{2m^2}{D-2}\right) I_{2,0}, \\ I_{2,1} = -\dfrac{1}{4m^2-s} I_{2,0} + \dfrac{D-3}{4m^2-s} I_{1,1}, \\ \quad \dots \end{cases} \tag{2.41}$$

2.5 Differential Equations for Feynman Integrals

In the previous section we have seen that we can find the MIs of a given family through an integral reduction. In this section we review a method to evaluate the MIs either analitically or numerically [15, 16], especially when their expression is complicated. This approach is based on differential equations for the MIs of an integral family. We present differential equations (DEs) starting from the massive bubble integral we computed before, then we will write down the general strategy, reviewing the following references [19, 30].

In order to write DEs for MIs we have to identify the variables with respect to which we differentiate, taking into account that FIs are analytic functions of invariants such as masses m_i and kinematic quantities (e.g. Mandelstam invariants). If we define x to be one of these invariants, using the fact that derivatives of MIs are integrals within the same family, we can write

$$\partial_x G_j = \sum_k h^{(x)}_{jk} I_k, \tag{2.42}$$

for some matrix coefficients $h^{(x)}_{jk}$. Now, since $\{I_k\}$ are reduced to $\{G_k\}$, i.e. $I_k = \sum_l c_{kl} G_l$, we get

$$\partial_x G_j = \sum_k A^{(x)}_{jk} G_k, \tag{2.43}$$

where $A^{(x)}_{jk} \equiv \sum_l h^{(x)}_{jl} c_{lk}$.

To be clearer, we write down the DEs for the massive bubble integral example, recalling the family definition (2.30) and its MIs $\{I_{1,0}, I_{1,1}\}$. In this case, our integrals depend only on two invariants, namely $I_{a_1,a_2} = I_{a_1,a_2}(m^2, s)$. We can compute straightforward derivatives with respect to m^2

$$\partial_{m^2} I_{a_1,a_2} = a_1 I_{a_1+1,a_2} + a_2 I_{a_1,a_2+1}. \tag{2.44}$$

Thus, for the two MIs, we get

$$\partial_{m^2} \begin{pmatrix} I_{1,0} \\ I_{1,1} \end{pmatrix} = \begin{pmatrix} I_{2,0} \\ 2I_{1,2} \end{pmatrix}. \tag{2.45}$$

If we use eq. (2.37), we can write

$$\partial_{m^2} \begin{pmatrix} I_{1,0} \\ I_{1,1} \end{pmatrix} = \begin{pmatrix} \frac{D-2}{2m^2} & 0 \\ -\frac{D-2}{m^2(4m^2-s)} & \frac{2(D-3)}{4m^2-s} \end{pmatrix} \begin{pmatrix} I_{1,0} \\ I_{1,1} \end{pmatrix} = A^{(m^2)} \begin{pmatrix} I_{1,0} \\ I_{1,1} \end{pmatrix}. \tag{2.46}$$

Analogously, using $\partial_s = \frac{1}{2s} p^\mu \partial_{p^\mu}$, we get the DE for the invariant s

$$\partial_s \begin{pmatrix} I_{1,0} \\ I_{1,1} \end{pmatrix} = \begin{pmatrix} 0 & 0 \\ \frac{D-2}{(4m^2-s)s} & -\frac{1}{2}\left(\frac{1}{s} + \frac{D-3}{4m^2-s}\right) \end{pmatrix} \begin{pmatrix} I_{1,0} \\ I_{1,1} \end{pmatrix} = A^{(s)} \begin{pmatrix} I_{1,0} \\ I_{1,1} \end{pmatrix}. \tag{2.47}$$

2.5.1 Mass Dimension and Integrability

Before proceeding in the computation of the DEs, let us make some observations on what we have computed so far. Firstly, we notice that, from eq. (2.30), I_{a_1,a_2} has mass dimension $[I_{a_1,a_2}] = D - 2a_1 - 2a_2$, so that, for some adimensional function g:

$$I_{a_1,a_2}(m^2, s; D) = m^{D-2a_1-2a_2} g(s/m^2; D). \tag{2.48}$$

Thus we can write the following DE

$$(s\partial_s + m^2\partial_{m^2}) I_{a_1,a_2} = (D/2 - a_1 - a_2) I_{a_1,a_2}. \tag{2.49}$$

So, if we apply this to our MIs, using eqs. (2.46),(2.47), we obtain a DE in diagonal form:

$$(s\partial_s + m^2\partial_{m^2}) \begin{pmatrix} I_{1,0} \\ I_{1,1} \end{pmatrix} = \frac{1}{2} \begin{pmatrix} D-2 & 0 \\ 0 & D-4 \end{pmatrix} \begin{pmatrix} I_{1,0} \\ I_{1,1} \end{pmatrix}. \tag{2.50}$$

The second observation consists in verifying the integrability of our system. This is achieved by checking the commutativity of partial derivatives, i.e. $\partial_s \partial_{m^2} - \partial_{m^2} \partial_s = 0$.

In our case,

$$[\partial_s A^{(m^2)} - \partial_{m^2} A^{(s)} + A^{(m^2)} A^{(s)} - A^{(s)} A^{(m^2)}] \begin{pmatrix} I_{1,0} \\ I_{1,1} \end{pmatrix} = 0. \tag{2.51}$$

One can substitute the explicit expressions obtained in eqs. (2.46), (2.47) for $A^{(m^2)}$ and $A^{(s)}$ and verify that the resulting matrix vanishes. However, when eq. (2.51) fails, it could signal that the reduction is incomplete.

2.6 Canonical Form

In this section we review the concept of the *canonical form* (or ϵ-form) [31]. Although the specific reduction procedures discussed in Chapters 4 and 5 do not strictly rely on this framework, the canonical form represents a natural and significant development in the theory of DEs for FIs. As such, it is included here to provide a complete theoretical background, though it is not required for the understanding of the subsequent original results in Chapters 4 and 5.

Intuitively, the idea behind the concept of ϵ-form tells us that, when we choose a basis of MIs such that the ϵ dependence is fully factorized

$$A^{(x)}_{jk}(\epsilon, x) = \epsilon \tilde{A}^{(x)}_{jk}(x), \tag{2.52}$$

integrating order by order in ϵ is easier. In other words, ϵ-form is convenient since, if we Laurent expand a vector of MIs

$$\vec{G} = \epsilon^{min} \sum_{k=1}^{\infty} \vec{G}^{(k)} \epsilon^k, \tag{2.53}$$

we can write

$$\begin{cases} \partial_x \vec{G}^{(0)} = 0 \Rightarrow \vec{G}^{(0)} = \vec{C}_0, \\ \partial_x \vec{G}^{(1)} = \tilde{A}(x) \vec{G}^{(0)} \Rightarrow \vec{G}^{(1)} = \int \tilde{A}(x) \vec{C}_0 + \vec{C}_1, \\ \qquad \dots \end{cases} \tag{2.54}$$

and we can integrate order by order in ϵ.

To begin with, we have to understand deeply the meaning of the parameter ϵ. In order to do this we recall that, in general, in FIs computations we encounter trascendental numbers and functions, such as powers of π in the integral measure or logarithms in the result of a scattering amplitude. We can study, from a systemic point of view, the importance of what trascendental functions give rise to.

Thus, we define a parameter, the so called *trascendental weight* [32], which keeps count of the "trascendentality" of a given expression. For example, rational numbers

or polynomials will have weight zero, while π and log will have weight one. Another example is the n-th *polylogarithm* $\mathrm{Li_n}(x)$ defined as

$$\mathrm{Li_n}(x) \equiv \sum_{k\geq 1} \frac{x^k}{k^n},\ n = 1, 2, \dots \tag{2.55}$$

which has trascendental weight n. If we focus on the *dilogarithm* Li_2, recurrent in FIs computations, we see that it has an equivalent definition:

$$\mathrm{Li_n}(x) = -\int_0^x \frac{\mathrm{d}\,t}{t} \log(1-t), \tag{2.56}$$

from which

$$\begin{cases} \partial_x \mathrm{Li}_2(x) = -\dfrac{1}{x}\log(1-x), \\ x\partial_x \mathrm{Li}_2(1-x) = \dfrac{1}{1-x}\log(x). \end{cases} \tag{2.57}$$

In general we can write

$$x\partial_x \mathrm{Li}_n(x) = \mathrm{Li}_{n-1}(x), \quad n > 2. \tag{2.58}$$

This definition for $\mathrm{Li_n}(x)$ can be viewed as an iteration of integrals over specific logarithmic integration kernels, namely $\frac{\mathrm{d}\,x}{x}$ and $\frac{\mathrm{d}\,x}{x-1}$. Thus we can interpret the trascendental weight as the number of integrations we have to perform in this integral representation. Now, we can view these functions under a DEs approach, by defining a weight-counting parameter ϵ (for the moment consider it unrelated to the dimensional regularisation parameter) with assigned weight -1. Thus we can define a zero weight vector

$$\vec{g}(x;\epsilon) = \begin{pmatrix} \epsilon^2 \mathrm{Li}_2(x) \\ \epsilon \log(x) \\ 1 \end{pmatrix}. \tag{2.59}$$

In particular, $\vec{g}(x;\epsilon)$ satisfies the following DE:

$$\partial_x \vec{g}(x;\epsilon) = \epsilon\left(\frac{A_0}{x} + \frac{A_1}{x-1}\right)\vec{g}(x;\epsilon), \tag{2.60}$$

with

$$A_0 = \begin{pmatrix} 0 & 0 & 0 \\ 0 & 0 & 1 \\ 0 & 0 & 0 \end{pmatrix}, \quad A_1 = \begin{pmatrix} 0 & -1 & 0 \\ 0 & 0 & 0 \\ 0 & 0 & 0 \end{pmatrix}. \tag{2.61}$$

We can rewrite eq. (2.60) in differential form as

$$d\vec{g}(x;\epsilon) = \epsilon\big[A_0\,\mathrm{dlog}(x) + A_1\,\mathrm{dlog}(1-x)\big]\vec{g}(x;\epsilon). \tag{2.62}$$

Notice that $\vec{g}(x;\epsilon)$ has weight zero. In fact, ϵ and $\mathrm{d} \equiv \mathrm{d}\, x\partial_x$ have weight -1, while log has weight +1. Given eq. (2.59), we can also express $\vec{g}$ as a series in powers of ϵ

$$\vec{g}(x;\epsilon) = \sum_{k\geq 0} \epsilon^k \vec{g}^{(k)}(x). \tag{2.63}$$

Plugging this ansatz in eq.(2.60) we can read, for the first few orders in ϵ:

$$\begin{cases} \partial_x \vec{g}^{(0)}(x) = 0, \\ \partial_x \vec{g}^{(1)}(x) = A(x)\vec{g}^{(0)}, \\ \partial_x \vec{g}^{(2)}(x) = A(x)\vec{g}^{(1)}. \end{cases} \tag{2.64}$$

Thus we have seen how to obtain eq. (2.54) for a basis of MIs by introducing the concept of trascendental weight.

2.6.1 Gauge Invariance of Differential Equations

When we study DEs of the form

$$\partial_x \vec{f}(x,\epsilon) = A(x,\epsilon)\vec{f}(x,\epsilon), \tag{2.65}$$

we may ask if they have a unique solution. To examine that, we consider an invertible matrix $T(x,\epsilon)$ such that, performing a change of basis yields

$$\vec{f} = T\vec{g}. \tag{2.66}$$

In the new basis, we have a similar DE

$$\partial_x \vec{g}(x,\epsilon) = B(x,\epsilon)\vec{g}(x,\epsilon), \tag{2.67}$$

where

$$B = T^{-1}AT - T^{-1}\partial_x T. \tag{2.68}$$

We have just proved the non-uniqueness, in a "gauge dependent" way. In fact, the matrix $A(x,\epsilon)$ tranforms to $B(x,\epsilon)$ under a gauge transformation. Therefore, we are allowed to write the solution of eq. (2.65) as a path ordered exponential

$$\vec{f}(x) = \mathbf{P}\exp\left[\int_{\mathcal{C}} A(x')dx'\right]\vec{f}(x_0), \tag{2.69}$$

where $\mathbf{P}$ stands for the path ordering along the path $\mathcal{C}$ connecting the base point x_0 to x. In particular, the operator $\mathbf{P}$ emerges as the time ordering operator in quantum mechanics. It can also be interpreted, in advanced quantum field theory, as a *Wilson line* [33] connecting two points x_0 and x along a contour $\mathcal{C}$.

Finally, another important property introduces the concept of *discontinuity*. In particular, let us assume that there exists another path $\mathcal{C}'$ that differs from $\mathcal{C}$ by a contour encircling a pole of A and it is still a solution of eq. (2.69). Thus, the path associated to the difference between $\mathcal{C}$ and $\mathcal{C}'$, which corresponds to taking a discontinuity of $\vec{f}$, will be a solution too. For example, if we consider the DE (2.60) and define two contours $\{\mathcal{C}, \mathcal{C}'\}$ such that $\mathcal{C}'$ crosses the branch cut starting from $x = 0$, we get, for $\{x \in \mathbb{C} \quad | \quad x < 0\}$:

$$\text{Disc}_{x=0}\,\vec{f}(x) = \left\{\mathbf{P}\exp\left[\int_{\mathcal{C}} A(x')dx'\right] - \mathbf{P}\left[\int_{\mathcal{C}'} A(x')dx'\right]\right\}\vec{f}(x_0) = 2\pi i \begin{pmatrix} -\log(1-x) \\ 1 \\ 0 \end{pmatrix}. \tag{2.70}$$

This property of discontinuities will be useful in further FIs analysis.

2.6.2 Symbols, Letters and Alphabets

As we stated in previous subsections, we often have to deal with special functions like logarithms or dilogarithms. We introduce a method to study important properties of special functions, called *symbol method* [34]. The idea behind this is the following: symbols preserves the information on the integration kernels, disregarding integration constants. Moreover, we define *letters* the integration kernels and their ensemble is called *alphabet*. For example, recall eq. (2.62), in this case the associated alphabet has two letters: $\{x, 1-x\}$. Intuitively, given the dilogarithm

$$\text{Li}_2(x) = -\int_0^x \text{dlog}(y)\int_0^y \text{dlog}(1-z), \tag{2.71}$$

we group the arguments of the logarithmic integration kernels in the symbol

$$\mathcal{S}(\text{Li}_2(x)) = -\big[1-x, x\big]. \tag{2.72}$$

An alternative notation is

$$\mathcal{S}(\text{Li}_2(x)) = -(1-x)\otimes x. \tag{2.73}$$

Notice that, inside the symbol, the order of integration kernels is opposite with respect to the one in the integral representation. We are now ready to give a formal definition for a generic symbol $\mathcal{S}$. Let $f^{(w)}$ be a uniform weight function (of weight w) whose derivative is given by

$$\text{d}\, f^{(w)} = \sum_i c_i f_i^{(w-1)}\,\text{dlog}\,\alpha_i, \tag{2.74}$$

where c_i are kinematic-independent constants, $f_i^{(w-1)}$ are uniform weight-$(w-1)$ functions and α_i are kinematic-dependent algebraic expressions. We define the symbol $\mathcal{S}$ of $f^{(w)}$ to be

$$\mathcal{S}(f^{(w)}) = \sum_i c_i[\mathcal{S}(f^{(w-1)}), \alpha_i]. \tag{2.75}$$

In particular, at weight 0, we define the empty symbol

$$[\quad] \equiv \mathcal{S}(1). \tag{2.76}$$

As a simple example one could write $\mathcal{S}(\log x) = [x]$ and for the dilogarithm: $\mathcal{S}(\mathrm{Li}_2(x)) = -\big[1-x, x\big]$, as we wrote above. The symbol satisfies the following properties:

$$\begin{aligned} [\dots, ab, \dots] &= [\dots, a, \dots] + [\dots, b, \dots], \\ [\dots, x^c, \dots] &= c[\dots, x, \dots], \\ [\dots, c, \dots] &= 0, \quad \text{if } c = \text{constant}. \end{aligned} \tag{2.77}$$

Another interesting property regards differentiation and discontinuities. Specifically, if we take the discontinuity across the negative real axis of $\log x$, whose symbol is $[x]$, it corresponds to set $[x] \to 1$. In general:

$$\begin{aligned} \mathrm{d}[a_1, \dots, a_{n-1}, a_n] &= \mathrm{dlog}(a_n)[a_1, \dots, a_{n-1}], \\ \mathrm{Disc}[a_1, a_2, \dots, a_n] &= \mathrm{Disc}(\log a_1)[a_2, \dots, a_n]. \end{aligned} \tag{2.78}$$

Thus, the symbol makes the branch cut structure and derivatives of a function manifest.

2.6.3 Generalization of the Canonical DEs Concept

In previous subsections we have seen how to build DEs for the massive bubble family. If we aim to extend this formalism to FIs, we have to take into account that FIs depend on kinematic variables and masses, thus a generalisation is needed. To begin with, we focus on the matrix A appearing in

$$\partial_x \vec{f}(x, \epsilon) = A(x, \epsilon)\vec{f}(x, \epsilon). \tag{2.79}$$

In general, we can choose a basis of MIs of the integral family so that the system is expressed in the so-called *canonical form*:

$$\mathrm{d}\, \vec{f}(\vec{x}, \epsilon) = \epsilon\, \mathrm{d}\, \tilde{A}(\vec{x})\vec{f}(\vec{x}). \tag{2.80}$$

In common cases, the connection matrix $\mathrm{d}\, \tilde{A}$ can be written in terms of dlog-type integration kernels:

$$\mathrm{d}\,\vec{f}(\vec{x},\epsilon) = \epsilon \sum_k A_k \,\mathrm{dlog}[\alpha_k(\vec{x})]\vec{f}(\vec{x},\epsilon), \tag{2.81}$$

where $\vec{x}$ is a set of variables and the set of letters $\{\alpha(\vec{x})\}$ is the alphabet of the problem. We call eq. (2.81) *canonical form* of the DEs for logarithmic integration kernels. Furthermore, it is crucial to highlight that A_k are purely numerical matrices, thus all the kinematic dependence is encoded in the letters $\alpha_k(\vec{x})$. Finally, we can even define a more general canonical form, in which the connection matrix $A(x)$ is not written as sum of logarithms:

Now, recall that the exact expression of the matrix $A(x,\epsilon)$ depends on the basis choice and in general it will have singularities. Let us consider the single-variable case and suppose that the system has a singularity at certain point x_k. It has been shown that a gauge transformation often exists such that the connection has only simple poles. In a single-variable case, this results in:

$$A(x) = \sum_k \frac{A_k}{x - x_k}. \tag{2.82}$$

Correspondingly, the differential (2.81) simplifies to:

$$\mathrm{d}\,\vec{f}(x,\epsilon) = \epsilon\left[\sum_k A_k \,\mathrm{dlog}(x - x_k)\right]\vec{f}(x,\epsilon). \tag{2.83}$$

However, FIs often involve more intricate arguments. For instance, in the massive bubble integral, the alphabet involves square roots of the kinematics, such as:

$$\alpha = \frac{\sqrt{1 - 4m^2/s} - 1}{\sqrt{1 - 4m^2/s} + 1}. \tag{2.84}$$

Such expressions suggest that the "canonical" variables are not always the physical invariants, but rather transcendental maps of them.

In conclusion, before proceeding with the massive bubble integral example, we can understand now that the weight counting parameter is precisely the ϵ in dimensional regularisation, with trascendental weight -1. In fact, in quantum field theory computations we encounter poles of the form $1/\epsilon$, which can be rewritten as $\log\Lambda$ for some cutoff Λ, hence we can naturally identify them.

2.6.4 Canonical DEs for the Massive Bubble

In previous subsections we have derived formally and generally all the necessary tools to analyze our example (2.30). In particular, we wrote down the DEs for the massive bubble integral with respect to m^2 and s respectively (see eqs. (2.46), (2.47)). We can

assume, only for this case, that $D = 2 - 2\epsilon$. We also review in A another example of derivation and solution of the system of DEs of the one-loop massless box integral family, presented in [19, 30].

It is easy to notice that these equations are not in canonical form (they contain ϵ^0 terms). In order to put them in ϵ-form we need to get rid of the unwanted ϵ^0. Firstly, we define a vector containing our chosen MIs

$$\vec{g} = \begin{pmatrix} I_{1,0} \\ I_{1,1} \end{pmatrix}. \tag{2.85}$$

Then we perform a change of basis, for a suitable matrix T:

$$\vec{f} = T\vec{g}. \tag{2.86}$$

If we require that the $A^{(x)}$ matrix is free of ϵ^0 terms (with $x = m^2, s$), employing also eqs. (2.65), (2.68), we get

$$\partial_{m^2} T = -T \begin{pmatrix} 0 & 0 \\ 0 & -\frac{2}{4m^2-s} \end{pmatrix}, \quad \partial_s T = -T \begin{pmatrix} 0 & 0 \\ 0 & \frac{s-2m^2}{s(4m^2-s)} \end{pmatrix}. \tag{2.87}$$

This leads to

$$T = \begin{pmatrix} 1 & 0 \\ 0 & \sqrt{(-s)(4m^2-s)} \end{pmatrix}. \tag{2.88}$$

Hence, in the new basis we obtain

$$\vec{f} = \begin{pmatrix} I_{1,0} \\ \sqrt{(-s)(4m^2-s)} I_{1,1} \end{pmatrix}. \tag{2.89}$$

For $m^2 > 0$ and $s < 0$ we find

$$\partial_{m^2}\vec{f} = \epsilon \begin{pmatrix} -\frac{1}{m^2} & 0 \\ -\frac{2}{m^2\sqrt{(1-4m^2/s)}} & -\frac{4}{4m^2-s} \end{pmatrix} \vec{f}, \quad \partial_s \vec{f} = \epsilon \begin{pmatrix} 0 & 0 \\ \frac{2}{s(4m^2-s)} & \frac{1}{4m^2-s} \end{pmatrix} \vec{f}. \tag{2.90}$$

Basically we have two canonical DEs of the form

$$\partial_x \vec{f} = \epsilon A^{(x)} \vec{f}, \tag{2.91}$$

which can be combined as

$$\mathrm{d}\,\vec{f} = \epsilon(\mathrm{d}\,\tilde{A})\vec{f}, \tag{2.92}$$

where $\mathrm{d} = \mathrm{d}\,m^2\partial_{m^2} + \mathrm{d}\,s\partial_s$ and $\tilde{A}$ is defined such that $\partial_x \tilde{A} = A^{(x)}$. We find the solution

$$\tilde{A} = \begin{pmatrix} -\log(m^2) & 0 \\ -2\log\left(\frac{\sqrt{1-4m^2/s}-1}{\sqrt{1-4m^2/s}+1}\right) & -\log(4m^2-s) \end{pmatrix}. \tag{2.93}$$

The equation above is a specific case of eq. (2.81). We identify three alphabet letters:

$$\left\{m^2, \frac{\sqrt{1-4m^2/s}-1}{\sqrt{1-4m^2/s}+1}, 4m^2-s\right\}. \tag{2.94}$$

We are now ready to solve the DE for $\vec{f}$, based on eq. (2.69):

$$\vec{f}(\vec{x},\epsilon) = \mathbf{P}\exp\left[\epsilon\int_{\mathcal{C}} \mathrm{d}\,\tilde{A}(\vec{x'})\right]\vec{f}(\vec{x_0},\epsilon), \tag{2.95}$$

where $\vec{x} = (m^2, s)$, $\tilde{A}$ is given by eq. (2.93) and $\vec{f}(\vec{x_0},\epsilon)$ is a boundary vector at a given base point $\vec{x_0}$. Thus, in order to solve eq. (2.95) we need to fix the *boundary conditions*, which will consist in physical consistence requirements. The idea is to identify singular points from the alphabet letters (2.94), in order to study the behavior of $\vec{f}$ near these singularities, i.e. when the letters go to zero or infinity. From eq. (2.94) we easily see that the singularities are $s = \{0,\infty\}$, $m = \{0,\infty\}$ and $s = m^2$. We can choose $s = 0$ as boundary condition. We know that physically this limit is non singular, since it is equivalent to set $p = 0$ in eq. (2.30). Hence, eq. (2.89) becomes a tadpole integral solved using eq. (2.10) with $a = 1$ and $D = 2 - 2\epsilon$:

$$I_{1,0} = \Gamma(\epsilon)(m^2)^{-\epsilon}. \tag{2.96}$$

So, the boundary condition reads as

$$\vec{f}(s=0,m^2;D=2-2\epsilon) = \begin{pmatrix} \Gamma(\epsilon)(m^2)^{-\epsilon} \\ 0 \end{pmatrix}. \tag{2.97}$$

We rewrite the alphabet (2.94) with the change of variables $s = -m^2(1-x)^2/x$:

$$\left\{m^2, x, m^2\frac{(1+x)^2}{x}\right\}, \tag{2.98}$$

which can be written in terms of the independent variables only

$$\left\{m^2, x, 1+x\right\}. \tag{2.99}$$

In addition, we can get rid of the m^2 dependence, as it correndponds to an overall scale. Therefore we can either set $m^2 = 1$ or multiply all integrals by $m^{-2\epsilon}$. We make the final basis choice, with normalisation consistent with the selected boundary condition above

$$\vec{f}(x;\epsilon) \equiv \frac{1}{\Gamma(\epsilon)m^{-2\epsilon}} \begin{pmatrix} I_{1,0} \\ \sqrt{(-s)(4m^2-s)}I_{1,1} \end{pmatrix}. \tag{2.100}$$

Thus the final differential equation reads as

$$\mathrm{d}\,\vec{f}(x;\epsilon) = \epsilon\,\mathrm{d} \begin{pmatrix} 0 & 0 \\ -2\log x & \log\frac{x}{(1+x)^2} \end{pmatrix} \vec{f}(x;\epsilon). \tag{2.101}$$

The boundary condition $s = 0$ is realised when $x = 1$:

$$\vec{f}(x=1;\epsilon) = \begin{pmatrix} 1 \\ 0 \end{pmatrix}. \tag{2.102}$$

Now, eq. (2.101) is equivalent to

$$\partial_x \vec{f}(x;\epsilon) = \epsilon \left[\frac{1}{x} \begin{pmatrix} 0 & 0 \\ -2 & 1 \end{pmatrix} + \frac{1}{1+x} \begin{pmatrix} 0 & 0 \\ 0 & -2 \end{pmatrix} \right] \vec{f}(x;\epsilon). \tag{2.103}$$

We can solve this order by order in ϵ if we write

$$\vec{f}(x;\epsilon) = \sum_{k\geq 0} \epsilon^k \vec{f}^{\,(k)}(x). \tag{2.104}$$

We also notice that eq. (2.101) decouple order by order in ϵ and we can find explicit expressions for the first few orders

$$\begin{aligned} \vec{f}^{\,(0)}(x) &= \begin{pmatrix} 1 \\ 0 \end{pmatrix}, \\ \vec{f}^{\,(1)}(x) &= \begin{pmatrix} 0 \\ -2\log x \end{pmatrix}, \\ \vec{f}^{\,(2)}(x) &= \begin{pmatrix} 0 \\ 4\,\mathrm{Li}_2(-x) + 4\log x \log(1+x) - \log^2 x + \pi^2/3 \end{pmatrix}. \end{aligned} \tag{2.105}$$

In conclusion, if we plug this in eq. (2.100) we obtain

$$I_{\text{bubble}}(s, m^2; D = 2-2\epsilon) = \frac{\Gamma(1+\epsilon)m^{-2\epsilon}}{\sqrt{(-s)(4m^2-s)}} \left[-2\log\left(\frac{\sqrt{1-4m^2/s}-1}{\sqrt{1-4m^2/s}+1} \right) + \mathcal{O}(\epsilon) \right]. \tag{2.106}$$

2.6.5 Unitarity Cuts

In the previous subsection we presented an instructive method to solve DEs for FIs, focusing on the massive bubble diagram example (2.100). However, the construction of a canonical basis is not a unique process and often necessitates the combination of

various methodologies. The approach reviewed here regards *unitarity cuts*, which can be used also in the context of IBP relations [35].

In order to introduce this concept, we focus on the definition of a generic propagator, whose imaginary part reads as

$$\mathrm{Im}\left[\frac{1}{p^2-m^2+i\epsilon}\right]=\frac{1}{2i}\left(\frac{1}{p^2-m^2+i\epsilon}-\frac{1}{p^2-m^2-i\epsilon}\right). \tag{2.107}$$

One can verify that the equation above vanishes when $\epsilon \to 0$, except for $p^2 \to m^2$. Thus, we report the general result

$$\mathrm{Im}\left[\frac{1}{p^2-m^2+i\epsilon}\right]=-\pi\delta(p^2-m^2), \tag{2.108}$$

which says that the propagator is real except for when the particle goes on-shell. In addition, eq. (2.107) highlights that the propagator has a discontinuty

$$\mathrm{Disc}\left(\frac{1}{p^2-m^2}\right)=2\pi i\int \mathrm{d}\,p\delta(p^2-m^2). \tag{2.109}$$

One can easily see that, from the equations above we can write

$$\frac{1}{p^2-m^2+i\epsilon}-\frac{1}{p^2-m^2+i\epsilon}\to -2\pi i\delta(p^2-m^2). \tag{2.110}$$

This relation can be rewritten equivalently as

$$\frac{1}{p^2-m^2}\to \delta(p^2-m^2). \tag{2.111}$$

The act of substituting the propagator with a δ-function as above is known as *cutting* that propagator. In other words, cutting a propagator means putting it on-shell as in eq. (2.108).

Furthermore, in a scattering amplitude we generally have more than one propagator and when we want to cut one of them we must apply Cutkosky rules [36, 37]. In particular, we define a *maximal cut* of an amplitude the act of putting the highest number of propagators on-shell.

We observe that, applying eq. (2.110) to a FI implies that the IBP structure is not affected by cuts, making the unitarity cut framework suitable in the context of an integral reduction. In particular the $\pm i\epsilon$ prescription is irrelevant for the differentiation, as presented in [35], thus making the IBPs for the propagators in eq. (2.110) unchanged with respect to the original propagator without the cut.

Let us review an other important consequence of unitarity cuts in the context of DEs, by analyzing again the bubble integral family (2.30) and their MIs $\{I_{1,0}, I_{1,1}\}$. Setting

$D = 2$ and applying an s-channel unitarity cut we obtain

$$\begin{aligned} I_{1,1} &= \int \frac{\mathrm{d}^2\, k}{i\pi} \frac{1}{[k^2 - m^2][(k+p)^2 - m^2]} \to \\ &\to \int \mathrm{d}^2\, k \delta(k^2 - m^2)\delta((k+p)^2 - m^2) = \frac{1}{\sqrt{(-s)(4m^2 - s)}}. \end{aligned} \tag{2.112}$$

This is an example of performing a maximal cut, since we put on-shell all the internal lines. Analogously, for the remaining MI $I_{1,0}$, we can write

$$I_{1,0} = \int \frac{\mathrm{d}^2\, k}{i\pi} \frac{1}{k^2 - m^2} \to \int \mathrm{d}^2\, k \delta(k^2 - m^2) = \pm 1. \tag{2.113}$$

This results are precisely the constant prefactor that we introduced in eq. (2.89) to write the DE in canonical from.

In conclusion, in this section we have briefly reviewed that the theory of unitarity cuts can play an important role in the context of integral reduction, both for the IBP computation and for the properties of DEs in their canonical basis.

Chapter 3

Baikov Representation and Syzygy Equations

In this chapter we discuss an alternative representation for loop integrals: the *Baikov representation* [5–7]. We will see that its main objective is to analyze integrals properties rather than evaluating them (which was the main purpose of Feynman representation). We will present also two different approaches to this new representation, namely the *standard* Baikov representation and the *loop-by-loop* Baikov representation [8], showing their benefits and drawbacks. The main difference between these two sub-representation is that in the standard one, the whole integral is parametrized simultaneously. Instead, in the loop-by-loop one, the integral is parametrized one loop at a time. The definitions and theoretical features of the Baikov representation presented in this chapter rely primarily on the framework developed in [38].

Moreover, we will also provide examples of the Baikov representation of two-loop diagrams. We also review the concept of *syzygy equations* [39] and discuss their role in the context of IBPs in Baikov representation.

3.1 Baikov Representation

In this section we review the *Baikov representation* and its variants. Their derivation can be found in [8, 40–43] and in B. The defining characteristics of this representation is that the integration variables are the propagators of the Feynman integral. We immediately notice that this representation has the advantage that performing unitarity cuts becomes a trivial operation. We recall that a unitarity cut, according to Cutkosky rules , requires the replacement of the cut propagator with a delta function [36]. Hence, a generalized cut becomes a residue operation, since in Baikov representation the propagators themselves are the integration variables.

An other useful feature of Baikov representation is the investigation of linear relations

between FIs, such as IBP identities, which turned out to be more transparent in this representation rather than in the Feynman one. Finally, before writing explicitly the representation, we should keep in mind that the main objective of Baikov representation is not to evaluate FIs. The reason for this is that, compared to Feynman parametrisation, the Baikov one usually has higher number of integration variables, more complicated defining polynomials and integration region.

3.1.1 Standard Baikov Representation

As we mentioned before, the standard Baikov representation consists in parametrizing the whole integral all at once. Let us recall the definition of an L-loop integral family in eq. (2.19).

We define the standard Baikov representation of $I_{a_1,\dots,a_n}$, the integral

$$I_{std} = \frac{\mathcal{J}(-i)^L \pi^{(L-n)/2} \mathcal{E}^{(-D+E+1)/2}}{\prod_{l=1}^{L} \Gamma((D+1-E-l)/2)} \int_{\mathcal{C}} \frac{\mathcal{B}^{(D-E-L-1)/2}}{z_1^{a_1} \dots z_n^{a_n}} \, \mathrm{d}^n z, \tag{3.1}$$

where $\{z_i\}_{i=1}^n$, called Baikov variables, represent the propagators of the family. In particular, the total number n (denoted as n_{std} in this case) of Baikov variables is defined as

$$n_{std} = \frac{L(L+1)}{2} + EL, \tag{3.2}$$

where E is the number of independent external momenta p_i. The number of Baikov variables n_{std} counts how many scalar products involving loop momenta k_j (of the form $k_i \cdot k_j$ or $k_i \cdot p_j$) we can write down. Then, $\mathcal{E}$ and $\mathcal{B}$ are called the *external Baikov polynomial* and the *Baikov polynomial* respectively. They are defined as the Gram determinants

$$\mathcal{E} = \det[G(p_1, \dots, p_E)], \quad \mathcal{B} = \det[G(k_1, \dots, k_L, p_1, \dots, p_E)], \tag{3.3}$$

where the Gram matrix $G = G(q_1, \dots, q_n)$ has elements $G_{ij} = q_i \cdot q_j$ To simplify the notation we define

$$\gamma = \frac{D-E-L-1}{2}. \tag{3.4}$$

Furthermore, the jacobian $\mathcal{J}$ of the change of variable from the independent scalar products to the Baikov variables is $\mathcal{J} = \pm 2^{L-n}$. Hence, we can absorb all the prefactors in an overall constant

$$C = C(D, L, E, n) \equiv \frac{\mathcal{J}(-i)^L \pi^{(L-n)/2}}{\prod_{l=1}^{L} \Gamma((D+1-E-l)/2)} \tag{3.5}$$

We can rewrite eq. (3.1) more compactly as

$$I_{std} = C\mathcal{E}^{\frac{-D+E+1}{2}} \int_{\mathcal{C}} \frac{\mathcal{B}^{\gamma}}{z_1^{a_1} \dots z_n^{a_n}} \, \mathrm{d}^n z. \tag{3.6}$$

Finally, the integration contour $\mathcal{C}$ for the one-loop case is defined as

$$\mathcal{C} = \left\{ x \in \mathbb{R}^n : \frac{\mathcal{B}(x)}{\mathcal{E}} > 0 \right\}. \tag{3.7}$$

We also observe that, if we define as P the number of actual (physical) propagators we have that it could be smaller than n, i.e. $P \leq n$. Thus, the set of propagators must incorporate a number

$$N_{extra} = n - P \tag{3.8}$$

of extra propagators, so that the total number of propagator-like objects is equal to n.

3.1.2 Loop-By-Loop Baikov Representation

Let us consider standard Baikov representation. Since n grows quadratically with L (see eq. (3.2)), the number of integration variables will be much larger than the number of physical propagators. This motivates the search for an alternative method for Baikov representation, the loop-by-loop Baikov representation, whose purpose is to keep N_{extra} smaller.

The key idea behind this representation is to apply the standard one in eq. (3.1) to one loop at a time. The loop-by-loop representation is independent of the loop ordering, meaning we can choose any loop to start the parametrization. For the one-loop case we can directly substitute $L = 1$ in eq. (3.1):

$$I_{1-loop} = \frac{\mathcal{J}_1 (-i) \pi^{-E/2} \mathcal{E}^{(-D+E+1)/2}}{\Gamma((D-E)/2)} \int_{\mathcal{C}} \frac{\mathcal{B}^{(\gamma-1)/2}}{z_1^{a_1} \dots z_{E+1}^{a_{E+1}}} \, \mathrm{d}^{E+1} z. \tag{3.9}$$

Applying the equation above recursively, we get

$$I_{lbl} = \frac{\mathcal{J} (-i)^L \pi^{(L-n)/2}}{\prod_{l=1}^{L} \Gamma((D-E_l)/2)} \int_{\mathcal{C}} \frac{1}{z_1^{a_1} \dots z_n^{a_n}} \left(\prod_{l=1}^{L} \mathcal{E}_l^{\frac{-D+E_l+1}{2}} \mathcal{B}_l^{\gamma_l} \right) \mathrm{d}^n z. \tag{3.10}$$

The structure of eq. (3.10) is similar to the standard case with L loops and n Baikov variables. However there are substantial differences, E_l is now the number of independent momenta external to the l-th loop, after having integrated out lower loops. Moreover, each loop will have its external Baikov polynomial and its Baikov polynomial $\mathcal{E}_l$ and $\mathcal{B}_l$

$$\mathcal{E}_l = \det[G(q_1, \dots, q_{E_l})], \quad \mathcal{B}_l = \det[G(k_l, q_1, \dots, q_{E_l})]. \tag{3.11}$$

In particular, the E_l momenta q_i, external to loop l, can be identified with the external momenta p_i, other loops momenta k_j or combinations of them. Moreover, for the L-th loop, the external polynomial $\mathcal{E}_L$ is always independent of Baikov variables, since it depends only on scalar products between the external momenta $p_i \cdot p_j$, thus it is taken out from the integral sign. In addition, note that $\mathcal{B}_l$ has

$$\gamma_l \equiv \frac{D - E_l - 2}{2} \tag{3.12}$$

as exponent. As in the standard case, we can define a constant C' absorbing all the prefactors

$$C' = C'(D, L, E, n) = \frac{\mathcal{J}(-i)^{L}\pi^{(L-n)/2}\mathcal{E}_L^{(-D+E_L+1)/2}}{\prod_{l=1}^{L}\Gamma((D-E_l)/2)}, \tag{3.13}$$

where the Jacobian $\mathcal{J}$ is $\mathcal{J} = \pm 2^{L-n}$.

Thus, we can express the parametrized integral as

$$I_{lbl} = C' \int_{\mathcal{C}} \frac{1}{z_1^{a_1} \dots z_n^{a_n}} \prod_{l=1}^{L-1} \mathcal{E}_l^{(-D+E_l+1)/2} \prod_{m=1}^{L} \mathcal{B}_m^{\gamma_m} d^n z. \tag{3.14}$$

The integration contour $\mathcal{C}$ is defined as

$$\mathcal{C} = \left\{ x \in \mathbb{R}^n : \bigcap_{l=1}^{L} \frac{\mathcal{B}_l}{\mathcal{E}_l} > 0 \right\}. \tag{3.15}$$

In other words, the integration region consists in the part of Baikov variables space corresponding to the integration regions of the L individual loops. In conclusion, the number n of integration variables is

$$n_{lbl} = L + \sum_{l=1}^{L} E_l. \tag{3.16}$$

It is natural to confront n_{lbl} and n_{std}, defined in eq. (3.2). Let us discuss the case for which $E_l = E + L - l$, i.e. when all loops have dependence on all external momenta and all loop momenta of higher loops. If we plug this expression of E_l in eq. (3.16), we get

$$n_{lbl} = n_{std}. \tag{3.17}$$

In this case, the standard and loop-by-loop representations are equivalent. There is no advantage in parametrizing the integral using the loop-by-loop method, as the number of extra propagators required is identical to that of the standard representation. Whereas, for all other cases we have

$$n_{lbl} < n_{std}, \tag{3.18}$$

which implies that, in general, it is more convenient to parametrize loop-by-loop, since our aim is to keep N_{extra} (see eq. (3.8)) smaller.

3.1.3 The Box-Triangle Diagram

In this subsection, we discuss an example of the strategy used to determine the loop ordering in a multi-loop diagram for writing the loop-by-loop Baikov representation. Specifically, we will focus on the different number of extra propagators that result from choosing one loop over another as the initial loop. Let us consider the massless two-loop box-triangle diagram in fig. 3.1, with loop momenta k_1, k_2 and external on-shell incoming momenta p_1, p_2, p_3, thus, $p_1^2 = p_2^2 = 0$.

Moreover, due to momentum conservation we have $p_1 + p_2 + p_3 = 0$. To simplify the notation from now on we will write $p_{ij} \equiv p_i + p_j$. We also define the only Mandelstam invariant for this diagram $s = p_{12}^2 = 2p_1 \cdot p_2$.

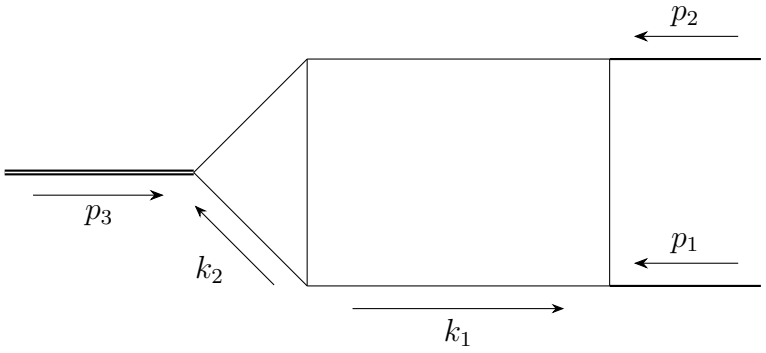

Figure 3.1: Box-triangle diagram with loop momenta k_1, k_2 and external legs p_1, p_2, p_3.

We identify six propagators

$$\begin{aligned} D_1 &= k_1^2, & D_2 &= k_2^2, \\ D_3 &= (k_1 + p_{12})^2, & D_4 &= (k_1 + k_2)^2, \\ D_5 &= (k_2 - p_{12})^2, & D_6 &= (k_1 + p_1)^2. \end{aligned} \tag{3.19}$$

This suggests that, in order to decrease the number of integration variables, we must pick k_2 as starting loop in the loop-by-loop representation. In fact, if we associate the loop $l = 1$ to the loop momentum k_2 we see that

$$n_{\text{lbl}} = \left[L + \sum_{l=1}^{L} E_l \right]_{L=2, E_1=2, E_2=2} = 6. \tag{3.20}$$

Notice that, if we parametrize starting from the k_2-loop, we do not need to add extra propagators, making it a more convenient representation, compared to the standard one. We discuss in detail this choice of loop ordering in Chapter 4, when we will present the integral reduction of the box-triangle family.

In order to highlight the advantages of the loop-by-loop representation, let us examine the other possible choice of loop ordering, for which the starting loop is the k_1-loop. Basically, we want to compute the Baikov polynomials $\{\mathcal{E}_l, \mathcal{B}_l\}$ for $l = 1, 2$, where the loop $l = 1$ is associated to the loop momentum k_1. We can compute n_{lbl} from eq. (3.16), in order to see how many extra propagators we should add to the six already found. In this case: $L = 2$, $E_1 = 3$, $E_2 = 2$, thus

$$n_{lbl} = 7. \tag{3.21}$$

It is straightforward to understand that we must add only one propagator. We identify it by rewriting all the D_i in the form $k_i \cdot k_j$ or $k_i \cdot p_j$ and look for the missing scalar product. However, in this case we can use symmetries to find the missing propagator. In this context, these missing propagators correspond to the ISPs we defined before. In fact, the set of propagators $\{D_i\}$ is invariant under the symmetry $k_1 \leftrightarrow -k_2$ if we add a propagator

$$D_7 = (k_2 - p_1)^2. \tag{3.22}$$

We are now ready to compute our polynomials, by using the free package `BaikovPackage`[38], available in `Mathematica`.

The first polynomial is

$$\mathcal{E}_1 = \det[G(p_1, p_2, k_2)], \tag{3.23}$$

since the external momenta to the k_1-loop are $E_1 = \{p_1, p_2, k_2\}$. Explicitly, with the change of notation $D_i \to z_i$, we obtain

$$\mathcal{E}_1 = -\frac{s}{4}(z_2 z_5 + s z_7 - z_2 z_7 - z_5 z_7 + z_7^2). \tag{3.24}$$

Then, $\mathcal{B}_1$ is defined as

$$\mathcal{B}_1 = \det[G(k_1, p_1, p_2, k_2)]. \tag{3.25}$$

Now, the k_1 is solved, there is still the k_2-loop to take care of, as we see in fig. 3.2.

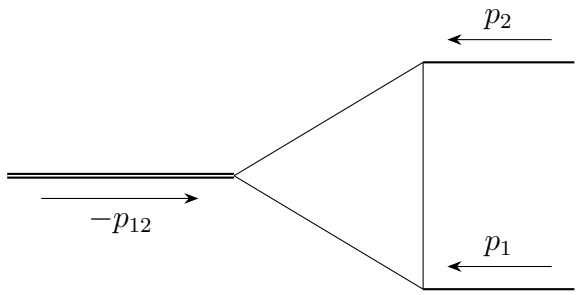

Figure 3.2: Box-triangle diagram after having integrated out the k_1-loop.

In this case, $E_2 = \{p_1, p_2\}$ and the Baikov polynomials are straightforward:

$$\mathcal{E}_2 = \det[G(p_1, p_2)] = -\frac{s^2}{4}, \quad \mathcal{B}_2 = \det[G(p_1, p_2, k_2)] = \mathcal{E}_1. \tag{3.26}$$

Note that, if we parametrized the diagram with the standard Baikov representation, we would have obtained

$$n_{std} = \frac{L(L+1)}{2} + EL\Big|_{L=2,E=2} = 7. \tag{3.27}$$

We immediately notice that, if we start the loop-by-loop parametrization with the k_1-loop, we get $n_{lbl} = n_{std}$, i.e. the number of Baikov variables is the same for both representations.

Finally, we can read off the general approach: in order to minimize N_{extra}, the optimal strategy consists in starting the loop-by-loop parametrization with the loop containing the fewest propagators and then proceed in increasing order. In fact in the box-triangle example, we have seen that $N_{extra} = 0$ if we start from the triangle-loop (see fig. 3.1). Whereas $N_{extra} = 1$ if we start from the box-loop.

3.1.4 The Double-Box Diagram

We present another example of loop-by-loop Baikov representation: the massless scalar double-box diagram with four external legs, showed in fig. 3.3. We denote the two loop momenta as k_1, k_2 and the external on-shell incoming momenta as p_i, with $i = 1, 2, 3, 4$.

Moreover, our loops have the same shape, since they are both boxes. In this case, the choice of the starting loop is completely arbitrary.

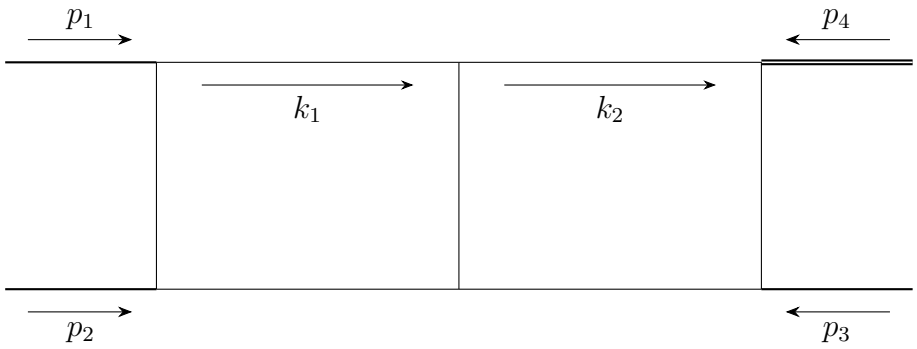

Figure 3.3: Double-box diagram with loop momenta k_1, k_2.

We see that the propagators are

$$\begin{aligned} D_1 &= k_1^2, & D_2 &= (k_1+p_1)^2, \\ D_3 &= (k_1+p_{12})^2, & D_4 &= k_2^2, \\ D_5 &= (k_2+p_{12})^2, & D_6 &= (k_2+p_{123})^2, \\ D_7 &= (k_1-k_2)^2. \end{aligned} \tag{3.28}$$

Let us start with the k_2-loop. We compute the total number of propagators

$$n_{\text{lbl}} = \left[L + \sum_{l=1}^{L} E_l\right]_{L=2,E_1=3,E_2=3} = 8. \tag{3.29}$$

Thus, we have to introduce only one ISP in the form of the extra propagator

$$D_8 = (k_1+p_{123})^2. \tag{3.30}$$

Hence, the Baikov polynomials $\mathcal{E}_l$, $\mathcal{B}_l$ will be functions of the Baikov variables $\{z_i\}_{i=1}^8$ and of the Mandelstam invariants (s,t) defined as

$$p_1\cdot p_2 = \frac{s}{2}, \quad p_2\cdot p_3 = \frac{t}{2}, \quad p_1\cdot p_3 = -\frac{s+t}{2}, \tag{3.31}$$

keeping in mind that we have three independent external momenta, due to momentum conservation. Thus we find expressions for the Baikov polynomials for k_2 loop ($l=1$) $\mathcal{E}_1(s,t,z_i)$, $\mathcal{B}_1(s,t,z_i)$.

After simplifying the k_2 loop we remain with the diagram in fig. 3.4.

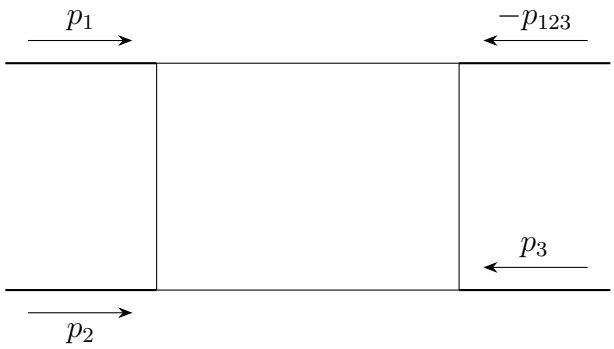

Figure 3.4: Double-box diagram after having integrated out loop momentum k_2.

Thus we can compute the Baikov polynomials for the k_1 loop ($l = 2$): $\mathcal{E}_2(s,t)$, $B_2(s,t,z_i)$. One can note that in general, we always have one external Baikov polynomial (specifically, the one computed once we are left with the one-loop form of the starting multi-loop diagram) which is independent from the Baikov variables z_i. In fact, when we parametrize loop-by-loop a given integral, the last loop reduction will have as external momenta only the ones external to the whole diagram, in fact

$$\mathcal{E}_2(s,t) = \det[G(p_1,p_2,p_3)] = -\frac{1}{4}st(s+t). \tag{3.32}$$

Therefore, we can generalize this observation by stating that, if we consider a generic L-loop diagram, we will have $2L-1$ Baikov and external Baikov polynomials depending on the variables z_i. This observation will be useful when we will combine the concepts of IBPs (seen in section 2.4) and syzygy equations in next section.

3.2 Syzygy Equations

In this section we discuss syzygy equations, a special kind of equations involving polynomials. They play a fundamental role in the determination of IBP relations for FIs, formulated using the Baikov representation. This review is based on the following references [13, 39, 44].

In general, let us consider a n-dimensional list of *known* polynomials

$$\vec{f}(\mathbf{z}) = \{f_1(\mathbf{z}), \ldots, f_n(\mathbf{z})\}, \tag{3.33}$$

and a n-dimensional list of *unknown* polynomials

$$\vec{g}(\mathbf{z}) = \{g_1(\mathbf{z}), \ldots, g_n(\mathbf{z})\}. \tag{3.34}$$

We define a *syzygy equation* for $\vec{f}(\mathbf{z})$, the equation

$$\vec{f}(\mathbf{z}) \cdot \vec{g}(\mathbf{z}) = \sum_{j=1}^{n} f_j(\mathbf{z}) g_j(\mathbf{z}) = 0, \tag{3.35}$$

where $\vec{g}(\mathbf{z})$ corresponds to the syzygy module $\vec{a}$ mentioned above, constituting a set of solutions for the syzygy equation.

Furthermore, if we consider a set of solutions

$$\{\vec{g}^{\,(1)}(\mathbf{z}), \ldots, \vec{g}^{\,(N)}(\mathbf{z})\}, \tag{3.36}$$

we can write any other solution as

$$\vec{g}(\mathbf{z}) = \sum_{j=1}^{N} p_j(\mathbf{z}) \vec{g}^{\,(j)}(\mathbf{z}), \tag{3.37}$$

where $p_k(\mathbf{z})$ are arbitrary polynomials. In general, we want to find a *minimal* set of generators $\{\vec{g}^{\,(j)}\}_j$, i.e. that they are independent of each other with respect to combination of the form in eq. (3.37). However, it is often unnecessary to find all the generators. Thus, we need to find only a subset of them, up to a maximum degree, depending on the problem we are analyzing.

We present briefly a way of finding solutions to syzygy equations, precisely via *linear constraints* a strategy successfully employed within the context of loop integrals [39]. In other words, we make an ansatz for $\vec{g}(\mathbf{z})$ up to a maximum degree: let us define a list of exponents $\alpha = (\alpha_1, \ldots, \alpha_n)$ so that a polynomial $\mathbf{z}^\alpha = (z_1^{\alpha_1}, \ldots, z_n^{\alpha_n})$ and $|\alpha| \equiv \sum_k \alpha_k$, then

$$\vec{g}(\mathbf{z}) = \sum_j \sum_{|\alpha| \leq d} c_{ja} \mathbf{z}^\alpha \hat{e}_j \tag{3.38}$$

will be a syzygy solution, with maximum degree d and with $\hat{e}_j$ being the unit vector in the j-th direction.

Now if we insert the ansatz in eq. (3.35) we basically obtain a linear system for the coefficients $c_{j\alpha}$, since we are imposing that the coefficient of each monomial in $\mathbf{z}$ vanishes. Since the linear system is homogeneous in $c_{j\alpha}$, we could have a non-trivial solution compatible with the ansatz. Roughly speaking, this solution constrains a subset of $c_{j\alpha}$ to be a linear combination of another subset called independent coefficients. In other words, we can write explicitly

$$c_{j\alpha} = \sum_{k,\beta} a_{jk\alpha\beta} c_{k\beta}, \tag{3.39}$$

where the dummy indices k, β identify the independent coefficients $c_{k\beta}$ and $a_{jk\alpha\beta}$ are rational functions depending on the specific problem we are dealing with. If we substitute eq. (3.39) in eq. (3.38), we obtain a list of syzygy solutions,by setting all independent coefficients but one to zero and the remaining one to an arbitrary non-zero value, for all possible choice of the independent coefficients.

Now, the obtained syzygy might not be all linear independent, especially when the polynomials p_j in eq. (3.37) are not constants. This means that we can map each known syzygy solution to a linear equation (with a one-to-one correspondence)

$$\sum_{j,\alpha} c_{j\alpha} \mathbf{z}^{\alpha} \hat{e}_j \leftrightarrow \sum_{j,\alpha} c_{j\alpha} y_{\alpha j} = 0, \tag{3.40}$$

where $y_{\alpha j}$ are the unknowns of these equations. We solve these equations (e.g., via Gaussian elimination), effectively removing any linear dependencies between syzygies.

3.2.1 IBPs in Standard Baikov Representation

In section 2.4 we have seen how to write IBPs between integrals in the momentum representation. We discuss now, how to generate them in Baikov representation, showing why it is more convenient to use this parametrization. That happens because, given a generic IBP for a multi-loop integral family as in eq. (2.19), the derivative term often produces integrals with increasing denominator powers a_i. These integrals, irrelevant for the integral reduction, drastically increase the size and complexity of our IBP system, making it a major computational bottleneck, in case of complicated multi-loop topologies. A solution to this problem is to approach IBPs from the viewpoint syzygy equations in the Baikov representation for the family [13, 45], since in this parametrisation the variable with respect to we differentiate are the propagator themeselves.

Recall the standard Baikov representation in eq. (3.6). Let us simplify the notation by setting

$$K \equiv C\mathcal{E}^{\frac{-D+E+1}{2}}, \tag{3.41}$$

thus eq. (3.6) becomes

$$I_{a_1,\dots,a_n} = K \int \mathrm{d}^n z \frac{\mathcal{B}^\gamma}{z_1^{a_1} \dots z_n^{a_n}}. \tag{3.42}$$

In standard Baikov representation, IBPs read as

$$0 = K \int \mathrm{d}^n z \sum_{i=1}^{n} \frac{\partial}{\partial z_i} \left(g_i(\mathbf{z}) \frac{\mathcal{B}^\gamma}{z_1^{a_1} \dots z_n^{a_n}} \right), \tag{3.43}$$

where $g_i(\mathbf{z})$ are chosen polynomials of $\mathbf{z}$. We obtain

$$0 = K \int \mathrm{d}^n z \sum_{i=1}^{n} \left(\frac{\partial g_i}{\partial z_i} + \frac{\gamma}{\mathcal{B}} g_i \frac{\partial \mathcal{B}}{\partial z_i} - a_i \frac{g_i}{z_i} \right) \frac{\mathcal{B}^\gamma}{z_1^{a_1} \dots z_n^{a_n}}. \tag{3.44}$$

We notice that the term proportional to $\frac{\partial \mathcal{B}}{\partial z_i}$ introduces a shift in the dimension D, in fact

$$\mathcal{B}^\gamma \to \mathcal{B}^{\gamma-1} \quad \Longrightarrow \quad D \to D - 2. \tag{3.45}$$

Moreover, the term proportional to $-a_i$ increases the powers of the propagators z_i, significantly expanding the IBP system and thus making the reduction more computationally demanding.

In order to solve these problems, we can interpret the polynomials $g_i(\mathbf{z})$ in the IBP relations as syzygy solutions. Specifically, let us suppose we can find polynomials $g_i(\mathbf{z})$ such that there exist polynomials $h_i(\mathbf{z}), h_0(\mathbf{z})$ satisfying the following syzygy equations

$$h_0(\mathbf{z})\mathcal{B} - \sum_{i=1}^{n} \left(g_i(\mathbf{z}) \gamma \frac{\partial \mathcal{B}}{\partial z_i} \right) = 0, \tag{3.46}$$

$$g_i(\mathbf{z}) = h_i(\mathbf{z}) z_i, \quad \text{for} \quad i \in \{j | a_j > 0\}. \tag{3.47}$$

In particular, eq. (3.46) has a closed form solution [46], whereas eq. (3.47) is already solved.

If we substitute the two equations above in eq. (3.43), using Leibniz rule for the derivative, we obtain

$$0 = K \int \mathrm{d}^n z \left[\sum_{i=1}^{n} \left(\frac{\partial g_i}{\partial z_i} - a_i \frac{g_i}{z_i} \right) - h_0 \right] \mathcal{B}^\gamma \frac{1}{z_1^{a_1} \dots z_n^{a_n}}. \tag{3.48}$$

The equation above generates IBPs via Baikov representation, avoiding both dimensional shift and higher power denominators. In other words, the h_0-term in eq. (3.48) absorbs

the $\mathcal{B}$ in the denominator of eq. (3.44), thanks to eqs. (3.46). Moreover, eq. (3.47) ensures that the term proportional to $-a_i$ does not contain higher powers of denominators.

Let us make another observation, eqs. (3.46) are syzygy equations for the set of generators

$$\left\{\mathcal{B}, \gamma\frac{\partial\mathcal{B}}{\partial z_1}, \ldots, \gamma\frac{\partial\mathcal{B}}{\partial z_n}\right\}. \tag{3.49}$$

In particular, their solutions will be the following vectors of polynomials

$$\{h_0, g_1, \ldots, g_n\}. \tag{3.50}$$

It is important to state that these solutions are not unique. In fact, as we have seen earlier, linear combinations of syzygies produce valid syzygy solutions.

3.2.2 The Massive Bubble Family

Before discussing the implementation of syzygy equations in the IBPs framework for the loop-by-loop representation, we review an instructive example of the standard Baikov case: the one-loop scalar massive bubble integral family, following the treatement presented in [23].

We follow two different paths to obtain the template equation: the first one is more pedagogical and uses an ansatz to find explicit syzygy solutions. The second approach, which will be used for further applications, is more general: it involves solving the syzygy equations for the polynomials $h_j = g_j/z_j$ rather than for g_j, following the intuition presented in [11]. We recall the massive bubble integral family

$$I_{a_1,a_2} = \int \frac{\mathrm{d}^D k}{i\pi^{D/2}} \frac{1}{D_1^{a_1} D_2^{a_2}}, \tag{3.51}$$

whose propagators D_1, D_2 have the following expression (with $p^2 = m^2$):

$$D_1 = k^2 - m^2, \quad D_2 = (k+p)^2, \tag{3.52}$$

where, as usual, k is the loop momentum and p is the external one. We delimit our analysis, recalling eq. (2.36), to the sector $s = \{1, 0\}$, i.e. we restrict the family to

$$I_{a_1,a_2}|_{a_2<0} = \int \frac{\mathrm{d}^D k}{i\pi^{D/2}} \frac{D_2^{-a_2}}{D_1^{a_1}}, \tag{3.53}$$

in order to reduce the family avoiding higher power denominators. The first step, as always, consists in computing the Baikov polynomial

$$\mathcal{B} = \det(G(k,p)) = k^2p^2 - (k\cdot p)^2, \tag{3.54}$$

writing it in terms of the Baikov variables $D_i \to z_i$. We get

$$\mathcal{B} = -\frac{1}{4}(z_1^2 + z_2^2) + \frac{1}{2}z_1 z_2 + m^2 z_2. \tag{3.55}$$

Looking at the syzygy condition in eq. (3.46), we have to impose

$$g_1 \frac{\partial \mathcal{B}}{\partial z_1} + g_2 \frac{\partial \mathcal{B}}{\partial z_2} = h_0 \mathcal{B}. \tag{3.56}$$

Next step consists in proposing an ansatz for the syzygy solutions

$$\begin{aligned} g_i &= c_{i0} + c_{i1} z_1 + c_{i2} z_2 \\ h_0 &= c_{00}. \end{aligned} \tag{3.57}$$

Imposing the condition above, fixes all c_{ij} except two of them. This means that we have two independent solutions, found by setting two free parameters, e.g. c_{12}, c_{22} to arbitrary values:

- $c_{12} \to 0$, $c_{22} \to 1$ leads to

$$\vec{g}^{\,(1)} = \begin{pmatrix} g_1^{(1)} \\ g_2^{(1)} \end{pmatrix} = \begin{pmatrix} 2z_1 + 2m^2 \\ z_1 + z_2 \end{pmatrix} = (2z_1 + 2m^2)\hat{e}_1 + (z_1 + z_2)\hat{e}_2. \tag{3.58}$$

- $c_{12} \to 1$, c_{22} leads to

$$\vec{g}^{\,(2)} = \begin{pmatrix} g_1^{(2)} \\ g_2^{(2)} \end{pmatrix} = \begin{pmatrix} z_2 - z_1 - 2m^2 \\ z_2 - z_1 \end{pmatrix} = (z_2 - z_1 - 2m^2)\hat{e}_1 + (z_2 - z_1)\hat{e}_2. \tag{3.59}$$

Now, in order to implement the other condition (see eq. (3.47)), it is useful to collect the coefficients of the syzygy solutions $\vec{g}^{\,(1)}, \vec{g}^{\,(2)}, z_2\vec{g}^{\,(1)}$ (recall that if we multiply a solution by a monomial, it is still a syzygy solution), into the following matrix

$$\left(\begin{array}{c|ccccccccc} & z_2\hat{e}_1 & \hat{e}_1 & z_1^2\hat{e}_1 & z_1 z_2 \hat{e}_1 & z_1\hat{e}_1 & z_1 z_2 \hat{e}_2 & z_2^2\hat{e}_2 & z_1\hat{e}_2 & z_2\hat{e}_2 \\ \hline \vec{g}^{\,(1)} & 0 & 2m^2 & 0 & 0 & 2 & 0 & 0 & 1 & 1 \\ \vec{g}^{\,(2)} & 1 & -2m^2 & 0 & 0 & -1 & 0 & 0 & -1 & 1 \\ z_2\vec{g}^{\,(1)} & 2m^2 & 0 & 0 & 2 & 0 & 1 & 1 & 0 & 0 \end{array}\right). \tag{3.60}$$

If we focus on the term proportional to $-a_i g_i / z_i$ in eq. (3.43), we realize that we have to solve the syzygy equations via Gaussian elimination, removing $z_2\hat{e}_1$ and $\hat{e}_1$ terms,

which would increase denominator powers in the sector $s = \{1, 0\}$. Thus, we remove the unwanted terms by finding a valid linear combination

$$C_1 \vec{g}^{\,(1)} + C_2 \vec{g}^{\,(2)} + C_3 z_2 \vec{g}^{\,(1)} = 0. \tag{3.61}$$

By solving this system, setting $C_3 = 1$, we find $C_1 = C_2 = -2m^2$, so that the new syzygy solution is

$$\vec{g}^{\,(\text{new})} = z_2 \vec{g}^{\,(1)} - 2m^2 \vec{g}^{\,(1)} - 2m^2 \vec{g}^{\,(2)} = \begin{pmatrix} 2z_1 z_2 - 2m^2 z_1 \\ z_2^2 + z_1 z_2 - 4m^2 z_2 \end{pmatrix}. \tag{3.62}$$

Therefore, since the condition (3.46) is valid for each solution g_i, we can compute explicitly h_0 for the new syzygy solution $\vec{g}^{\,(\text{new})}$

$$h_0 = \frac{1}{\mathcal{B}} \sum_{i=1}^{2} g_i^{(\text{new})} \frac{\partial \mathcal{B}}{\partial z_i} = 2z_2 - 4m^2. \tag{3.63}$$

Finally, plugging the expressions of h_0 and $g_i^{\,(\text{new})}$ we just computed in the master formula (3.43), we obtain the template equation

$$(1 - a_2) I_{a_1 - 1, a_2} + (1 + D - 2a_1 - a_2) I_{a_1, a_2 - 1} - 2m^2 (D - a_1 - 2a_2) I_{a_1, a_2} = 0. \tag{3.64}$$

In particular, the equation above is a template IBP identity that does not generate increased-power propagators for the sector $s = \{1, 0\}$. One can substitute specific values for (a_1, a_2) to find additional IBPs and the MIs for the integral family I_{a_1, a_2}.

As mentioned before, we could obtain eq. (3.64) by solving the syzygy equations for h_j. In particular, we have to solve the equation

$$h_0(\mathbf{z}) \mathcal{B} - \sum_{j=1}^{2} z_j h_j(\mathbf{z}) \gamma \frac{\partial \mathcal{B}}{\partial z_j} = 0. \tag{3.65}$$

The IBPs master formula (3.43), in terms of $h_j(\mathbf{z})$, becomes

$$0 = K \int \mathrm{d}^n z \sum_{j=1}^{2} \frac{\partial}{\partial z_j} \left(z_j h_j(\mathbf{z}) \mathcal{B}^{\gamma} \frac{1}{z_1^{a_1} z_2^{a_2}} \right) \tag{3.66}$$

Solving eq. (3.46) where $g(\mathbf{z})$ is replaced with eq. (3.47) yields:

$$\begin{cases} h_0 = (3 - D)(2m^2 - z_2) \\ h_1 = -2(m^2 - z_2) \\ h_2 = -4m^2 + z_1 + z_2, \end{cases} \tag{3.67}$$

where $\gamma = (D - 3)/2$. Now, substituting eq. (3.67) in eq. (3.66) we obtain the template equation (3.64).

3.3 Setup for an Integral Reduction

In this section we recall the necessary definitions to better structure an integral reduction, following the notation of [47]. As we stated in section 2.4, we divide the integral family into sectors, identified by the integers a_i. It is clear that integrals within the same sector share identical proper denominators, differing only in their exponents or numerators.

Among all the integrals in a given sector, we define the *corner integral* to be the only integral of the sector, whose exponents $\{a_i\}_{i=1}^n$ satisfy

$$a_i \in \{0, 1\}, \forall i. \tag{3.68}$$

From now on, we will identify a sector with the list of integers of its corner integral. Moreover, given an integral family $I_{\vec{a}} \equiv I_{a_1,\dots,a_n}$, if we denote a sector of this family as $S[I_{\vec{a}}]$ we can define a *subsector* $S[I_{\vec{b}}]$ if its set of non-vanishing integers $\vec{b}$ is a subset of $\vec{a}$ in the first sector. Thus, $S[I_{\vec{b}}]$ is a subsector of $S[I_{\vec{a}}]$ if they are not the same sector and if $b_i \leq a_i, \forall i$. Equivalently, we say that $S[I_{\vec{a}}]$ is a *parent sector* of $S[I_{\vec{b}}]$.

Since we focus exclusively on sectors within a given amplitude or form factor—specifically those satisfying a particular linear combination of proper denominators—it is practical to identify one or more *top sectors* for each family. Thus, the sector list for a family is restricted to these top sectors and their respective subsectors. We will consider only families with one top sector.

Moreover, we should also consider symmetries of the integrals, typically obtained via shifts of the loop momenta, which map integrals of different sectors into each other, this procedure is called *sector mapping*, and is crucial for the reduction. We can represent all the sectors contributing to an amplitude through a Feynman diagram. More in detail, we can draw the diagram of a scalar theory which is proportional to its corner integral.

Now, let us recall that the reduction to MIs consists in rewriting more complex integrals in the family as linear combinations of simpler ones, using the linear relations they satisfy. The definition of this complexity (*weight*) is not unique, we will use one of the most common conventions, namely we will focus on the following integers, that can be associated to a given Feynman diagram:

- the number t of proper denominators

$$t \equiv \sum_{i|a_i>0} 1, \tag{3.69}$$

- the total power r of proper denominators

$$r \equiv \sum_{i|a_i>0} a_i, \tag{3.70}$$

- the total power s of ISPs

$$s \equiv -\sum_{i|a_i \leq 0} a_i, \tag{3.71}$$

- the number u of higher power denominators, also known as number of *dots*

$$u \equiv r - t. \tag{3.72}$$

Chapter 4

Integral Reduction in Loop-by-Loop Baikov Representation

In this chapter we discuss the main algorithm behind the integral reduction of two-loop diagrams and its results. In particular, we apply the theoretical tools acquired in the previous chapters, in order to compute explicitly the MIs of two-loop scalar integral families. Specifically, we focus on the massless box-triangle family and the massless double-box family, introduced in 3.1.3 and 3.1.4 respectively. We recall that we always work in the loop-by-loop Baikov frame, since it is a suitable and convenient representation for the studying of FIs properties.

Moreover, we embed our IBP systems with the syzygy structure, in order to show how this method of performing the reduction lets us obtain the correct results for the MIs. We will compute the integral reduction with the syzygy method for two distinct cases:

- Solve the IBP system considering the *no dimensional shift* term in eq. (4.5).
- Take into account also the term in eq. (4.6) that avoids *higher powers of denominators*. We will see that in this case we need to compute the syzygy equations individually for each non-zero sector of the family.

Furthermore, we will follow two different paths to obtain the MIs:

- Compute the reduction with `FiniteFlow` [17, 48], implementing the identities via solving the syzygy equations using the `CALICO` package [44].
- Subsequently, the system is re-evaluated using the Laporta algorithm [18] as implemented in the `FFIntRed`[1] package.

[1] An in-house Mathematica package by Tiziano Peraro

The latter serves as an independent consistency check for the primary computation.

In the next section, we will present all the necessary tools to build the setup of an integral reduction, while in C we will explain in detail how the reduction is accomplished with `FiniteFlow`.

4.1 IBPs in Loop-by-Loop Baikov Representation

In this section we present the algorithm to be implemented in order to build IBPs in loop-by-loop Baikov representation. The structure of the problem is similar to the standard Baikov representation approach in, the main difference is that we have more Baikov polynomials to be differentiated with respect to the Baikov variables z_i. Let us consider a multi-loop integral family $I_{a_1,\ldots,a_n}$, its loop-by-loop representation is written as

$$I_{a_1,\ldots,a_n} = K' \int \mathrm{d}^n z \prod_{k=1}^{2L-1} \frac{\mathcal{B}_k^{\gamma_k}}{z_1^{a_1} \ldots z_n^{a_n}}. \tag{4.1}$$

In this notation, we denote by $\mathcal{B}_k$ those Baikov polynomials and external Baikov polynomials that depend explicitly on z_i. We also denote by γ_k their respective exponents. The external polynomial which depend only on the kinematics or other variables are absorbed in the constant prefactor K'. Except for that, the IBP relations are written following the standard Baikov steps. Hence,

$$0 = K' \int \mathrm{d}^n z \sum_{i=1}^{n} \frac{\partial}{\partial z_i} \left(g_i(\mathbf{z}) \prod_{k=1}^{2L-1} \frac{\mathcal{B}_k^{\gamma_k}}{z_1^{a_1} \ldots z_n^{a_n}} \right). \tag{4.2}$$

Thus we can write the syzygy equations, supposing that there exists polynomials $h_i(\mathbf{z})$, $h_0(\mathbf{z})$ such that

$$h_0 \prod_{k=1}^{2L-1} \mathcal{B}_k + \sum_{k=1}^{2L-1} \sum_{i=1}^{n} \left(g_i(\mathbf{z}) \gamma_k \frac{\partial \mathcal{B}_k}{\partial z_i} \prod_{j \neq k}^{2L-1} \mathcal{B}_j \right) = 0, \tag{4.3}$$

and

$$g_i(\mathbf{z}) = h_i(\mathbf{z}) z_i, \quad \text{for} \quad i \in \{j | a_j > 0\}. \tag{4.4}$$

Substituting in eq. (4.2) we obtain the master formula

$$0 = K' \int \mathrm{d}^n z \left(\sum_{i=1}^{n} \frac{\partial g_i}{\partial z_i} + h_0 - \sum_{i=1}^{n} a_i \frac{g_i}{z_i} \right) \prod_{k=1}^{2L-1} \frac{\mathcal{B}_k^{\gamma_k}}{z_1^{a_1} \ldots z_n^{a_n}}. \tag{4.5}$$

The equation above can be written in terms of $h_j(\mathbf{z})$:

$$0 = K' \int \mathrm{d}^n z \left\{ \sum_{i=1}^{n} \left[\frac{\partial (h_i z_i)}{\partial z_i} - a_i h_i \right] + h_0 \right\} \prod_{k=1}^{2L-1} \frac{\mathcal{B}_k^{\gamma_k}}{z_1^{a_1} \dots z_n^{a_n}}. \tag{4.6}$$

In particular, (4.5) generates identities both avoiding dimensional and higher powers in the denominators.

The decision to employ the loop-by-loop Baikov representation, rather than sticking to the standard approach, is motivated by the search of an alternative framework to extend the already existing method to perform an integral reduction in Baikov representation with syzygy equations. The standard parametrisation does not scale well: as the loop order increases, the number of Baikov variables grows, leading to an algebraic complexity that often makes reductions computationally demanding. Whereas, the loop-by-loop method can offer an improvement to this algorithm. By processing the family one loop at a time, we have a smaller number of ISPs with respect to the standard case, leading to a more compact IBP system, and to fewer integrals to be reduced. Combined with the use of syzygies, this strategy proved essential in bypassing the bottlenecks that usually make complex multi-loop calculations unmanageable.

The only drawback of this framework lies in the fact that we can not reduce integrals with more than one ISP. In order to overcome this issue one could apply transverse integration methods [47] or an alternative approach based on deriving the standard Baikov representation starting from the loop-by-loop one, by integrating the extra ISPs one by one, as presented in [38, 49, 50].

4.2 Integral Reduction of the Box-Triangle Family

In this section we present the integral reduction of the scalar two-loop massless box-triangle diagram, in the loop-by-loop Baikov representation. We aim to find the MIs by using IBP identities in the syzygy framework, using the master formulas (4.5) and (4.6).

We introduced the box-triangle diagram in section 3.1.3, we recall how it is drawn, in fig. 4.1.

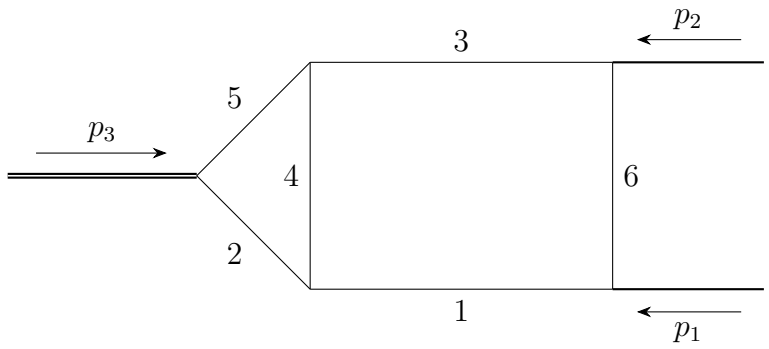

Figure 4.1: Box-triangle diagram with loop momenta k_1, k_2.

The six propagators are

$$\begin{aligned} D_1 &= k_1^2, & D_2 &= k_2^2, \\ D_3 &= (k_1 + p_{12})^2, & D_4 &= (k_1 + k_2)^2, \\ D_5 &= (k_2 - p_{12})^2, & D_6 &= (k_1 + p_1)^2. \end{aligned} \tag{4.7}$$

To begin with, we perform the loop-by-loop parametrisation, starting by the triangle loop (k_2-loop). It is crucial to highlight that with this representation we do not have extra propagators to be added, in other words, we do not have ISPs entering the game for the top sector.

We compute the Baikov polynomials, using `BaikovPackage` [38], obtaining:

$$\mathcal{E}_1 = -\frac{s}{4}(z_1 z_3 - z_3 z_6 - z_1 z_6 + s z_6 + z_6^2), \tag{4.8}$$

$$\begin{aligned} \mathcal{B}_1 = \frac{1}{4}\Big(& - s z_1 z_3 + s z_2 z_3 + z_1 z_2 z_3 - z_2^2 z_3 - z_2 z_3^2 - s^2 z_4 + s z_1 z_4 \\ & + s z_2 z_4 - z_1 z_2 z_4 + s z_3 z_4 + z_2 z_3 z_4 - s z_4^2 + s z_1 z_5 - z_1^2 z_5 \\ & - s z_2 z_5 + z_1 z_2 z_5 + z_1 z_3 z_5 + z_2 z_3 z_5 + s z_4 z_5 + z_1 z_4 z_5 - z_3 z_4 z_5 - z_1 z_5^2 \Big), \end{aligned} \tag{4.9}$$

$$\mathcal{E}_2 = -\frac{s^2}{4}, \tag{4.10}$$

$$\mathcal{B}_2 = \frac{1}{4}(-s^2 + 2 s z_1 - z_1^2 + 2 s z_3 + 2 z_1 z_3 - z_3^2). \tag{4.11}$$

After the polynomials computation, we are ready to write our syzygy equations, in order to build the IBP system. As we mentioned at the beginning of the chapter, we distinguish two cases of the syzygies computation: the no dimensional shift and the avoiding of higher powers of denominators.

4.2.1 No Dimensional Shift IBPs

We begin our analysis with the dimensional shift case. First of all, we have to solve the syzygy equation (4.3), in which the Baikov polynomials are $\{\mathcal{B}_k\}_{k=1}^{2L-1} = \{\mathcal{E}_1, \mathcal{B}_1, \mathcal{B}_2\}$. Note that we have excluded the external polynomial $\mathcal{E}_2$, since it does not depend on any Baikov variable.

Moreover, since in the no dimesional shift case the syzygy solutions does not depend on the choice of the sector we are analyzing, we compute them only for the top sector of the family.

In order to find the solutions $\{h_0, g_i\}$, we use the `CALICO` package [44], specifically the function `CATSyz`, which returns the generators of syzygy solutions of eq. (3.35). It is expressed as

$$g = \text{CATSyz}[\{f_1(\mathbf{z}), \dots f_n(\mathbf{z})\}, \{z_1, \dots z_n\}, d_{max}], \tag{4.12}$$

where d_{max} is the maximum degree of the solutions. The output g is a list containing at position $d+1$ all the found generators of degree d. In our case, according to eq. (4.3), we obtain the syzygy generators $\vec{g}(\mathbf{z})$ by substituting

$$\begin{cases} \vec{f}(\mathbf{z}) = \Big\{ -\prod_{k=1}^{2L-1} \mathcal{B}_k, \sum_{k=1}^{2L-1} \gamma_k \frac{\partial \mathcal{B}_k}{\partial z_1} \prod_{j\neq k}^{2L-1} \mathcal{B}_j, \dots, \sum_{k=1}^{2L-1} \gamma_k \frac{\partial \mathcal{B}_k}{\partial z_n} \prod_{j\neq k}^{2L-1} \mathcal{B}_j \Big\}, \\ \vec{g}(\mathbf{z}) = \{h_0, g_1, \dots, g_n\}. \end{cases} \tag{4.13}$$

Obviously the variables $\{z_i\}_{i=1}^n$ are the box-triangle propagators, thus $n = 6$. Lastly, we choose $d_{\max} = 3$, since no additional generators are found for higher degrees.

After finding the syzygy solutions, we implement eq. (4.5) to store our formal IBP relations, so that the integers a_i are kept symbolic. Moreover, by fixing the seed integrals to be all the integrals in the box-triangle family having maximum one dot and two ISPs, we store also explicit identities.

Now that we have generated and stored the identities, next step consists in solving them using `FFIntRed` and `FiniteFlow`, to find the MIs of the box-triangle family. In this framework, each integral is defined by the exponents a_i assigned to the correspondent propagator. For example, the complete diagram in fig. 4.1 represents the top sector

$$S_{\text{top}} = \{1, 1, 1, 1, 1, 1, 0\}. \tag{4.14}$$

Notice that the last entry in S_{top} must always be zero, since in this loop-by-loop representation we do not have the ISP needed in the standard representation. After the `FFIntRed` reduction we obtain the following three MIs:

$$G_{\text{TBox}} = \{G_k\}_{k=1}^3 = \{\{1, 1, 1, 0, 1, 0, 0\}, \{0, 1, 1, 1, 0, 0, 0\}, \{0, 1, 0, 1, 1, 1, 0\}\}. \tag{4.15}$$

We can draw the corresponding diagrams in fig. 4.2, considering that when we encounter a 0-entry, its associated propagator collapses to a point, i.e. it is *pinched*. For more details regarding the *Pinch Technique* (PT) see [51].

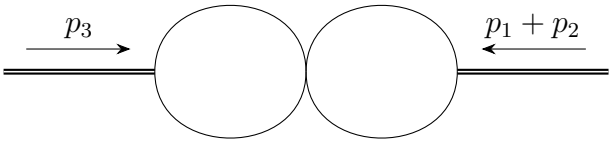

$$G_1 = \{1, 1, 1, 0, 1, 0, 0\}$$

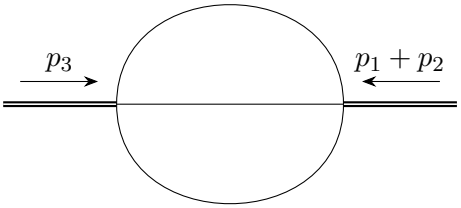

$$G_2 = \{0, 1, 1, 1, 0, 0, 0\}$$

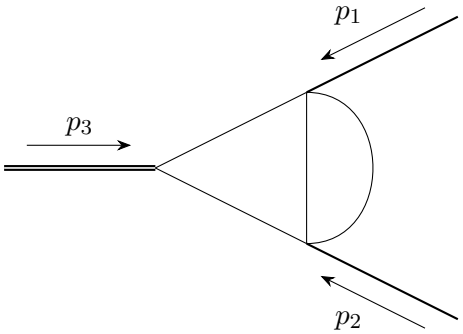

$$G_3 = \{0, 1, 0, 1, 1, 1, 0\}$$

Figure 4.2: Box-triangle MIs and their corresponding configurations.

Another important observation is that we must include mapping relations in our program, in fact, if we do not consider them we would get an additional master integral

$$G_4 = \{1, 0, 0, 1, 1, 0, 0\}, \tag{4.16}$$

whose corresponding diagram is depicted in fig. 4.3.

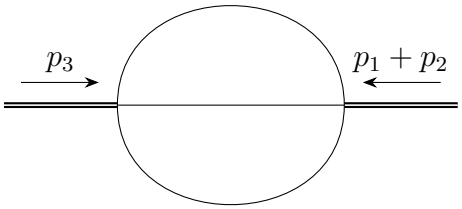

Figure 4.3: $G_4 = \{1, 0, 0, 1, 1, 0, 0\}$

However, we can see that G_4 is symmetric to the corresponding diagram of G_2, for some momenta shifting.

Furthermore, we verified, by generating the IBP equations explicitly with `FFIntRed` and solving them that the MIs are the ones of eq. (4.15). We can conclude that implementing syzygy equations with no dimensional shift in the construction of IBPs leads successfully to consistent results in the integral reduction obtained by Laporta algorithm.

4.2.2 No Higher Powers Denominators IBPs

In the following analysis we present the implementation of the integral reduction for the box-triangle family for the no higher powers in the propagators case. We will see that we have to treat the IBPs construction more carefully, since in this case we have to be sure that all the non-zero sectors of the family follow this condition. In other words, we need to find the syzygy solutions and generate the identities for each sector.

In order to do this, we notice that each corner integral in the sectors contains either actual propagators (*active propagators*) or ISPs (*inactive propagators*). For example, the sector $S[I_{1101100}]$ in fig. 4.4 is characterized by

$$\begin{cases} \text{active propagators} & = \{z_1, z_2, z_4, z_5\}, \\ \text{inactive propagators} & = \{z_3, z_6\}. \end{cases} \tag{4.17}$$

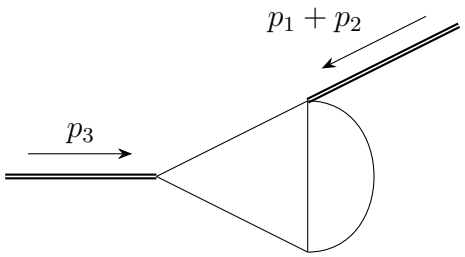

Figure 4.4: Feynman graph of the sector $S[I_{1101100}] = \{1, 1, 0, 1, 1, 0, 0\}$

We implement the IBP construction by rewriting the syzygy conditions (4.3), (4.4) in a convenient way, highlighting the difference between the active propagators and the ISPs. Specifically, if we define n_A as the number of active propagators in a given sector, we can split eq. (4.2) in two terms

$$\begin{aligned} 0 = K' \int \mathrm{d}^n z \Bigg\{ \sum_{i=1}^{n_A} \left[\frac{\partial (h_i z_i)}{\partial z_i} + \sum_{k=1}^{2L-1} \frac{\gamma_k}{\mathcal{B}_k} h_i z_i \frac{\partial \mathcal{B}_k}{\partial z_i} - a_i h_i \right] \\ + \sum_{j \neq n_A} \left[\frac{\partial g_j}{\partial z_j} + \sum_{k=1}^{2L-1} \frac{\gamma_k}{\mathcal{B}_k} g_j \frac{\partial \mathcal{B}_k}{\partial z_j} - a_j \frac{g_j}{z_j} \right] \Bigg\} \frac{\prod_{k=1}^{2L-1} \mathcal{B}_k^{\gamma_k}}{z_1^{a_1} \dots z_n^{a_n}}. \end{aligned} \tag{4.18}$$

We can see that for the active propagators we use the syzygy solution h_i, whereas for the ISPs we use the solution g_j. The physical meaning behind this choice lies in the fact that we want to avoid higher powers in the denominators only for the actual propagators of the diagram.

We can further simplify eq. (4.18) by rewriting the syzygy equation (4.3) as

$$h_0 B = \sum_{k=1}^{2L-1} \left[\sum_{i=1}^{n_A} h_i z_i \gamma_k \frac{\partial \mathcal{B}_k}{\partial z_i} + \sum_{j \neq n_A} g_j \gamma_k \frac{\partial \mathcal{B}_k}{\partial z_j} \right] \prod_{m \neq k} \mathcal{B}_m. \tag{4.19}$$

Then, eq. (4.18) becomes

$$0 = \int \mathrm{d}^n z \Bigg\{ \sum_{i=1}^{n_A} \left[\frac{\partial (h_i z_i)}{\partial z_i} - a_i h_i \right] + \sum_{j \neq n_A} \left[\frac{\partial g_j}{\partial z_j} - a_j \frac{g_j}{z_j} \right] + h_0 \Bigg\} \frac{\prod_{k=1}^{2L-1} B_k^{\gamma_k}}{z_1^{a_1} \dots z_n^{a_n}}. \tag{4.20}$$

Thus, following the equation above we can generate and store the IBPs to find the MIs as the previous case. We perform the reduction on the integrals with at most rank two and zero dots, setting the seed integrals to have maximum rank three and zero dots. This setup yields consistent outcomes with the previous case in eq. (4.15).

We can summarize in the steps below, the strategy to be followed in order to perform the reduction:

- Define the integral family.
- Parametrize loop-by-loop the family and compute the Baikov polynomials.
- Identify the non-zero sectors of the family.
- For each sector, after selecting the active propagators build the IBP identities using the syzygy solutions h_i.
- Generate the IBPs for the inactive ones, using the syzygy solutions g_i.

- Store the identities and find the MIs.

However, a natural question arises concerning if solving the syzygy equations for every individual sector is strictly necessary, given the associated computational cost. To examine this, we test whether employing the syzygy solutions h_i solely for the top sector represents an effective shortcut strategy.

It turns out that this approach remains consistent and successful, as the reduction still yields the complete set of MIs in eq. (4.15) without requiring the explicit solution of syzygies for the lower-level sub-sectors.

4.3 Integral Reduction of the Double-Box Family

In this section we present the integral reduction of the scalar two-loop massless double-box integral family, in the loop-by-loop Baikov representation framework, with four external momenta. We will follow analogous steps as in the box-triangle diagram, expecting a higher number of MIs, due to the fact that the double-box family has a more complex topology.

We recall the double-box structure cf. 3.1.4, pictured in fig 4.5.

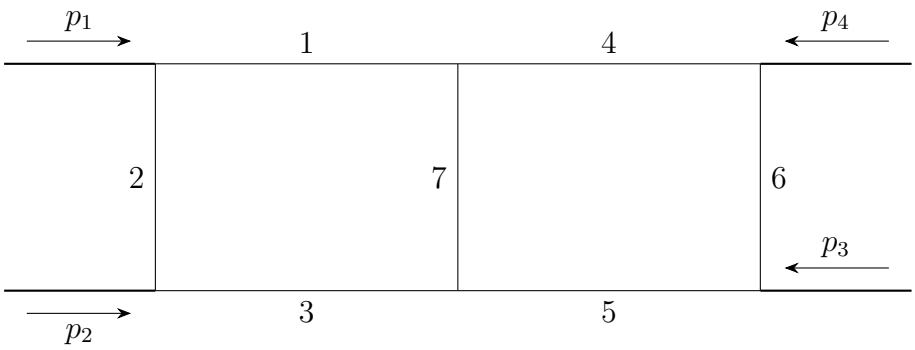

Figure 4.5: Double-box diagram with loop momenta k_1, k_2.

The propagators are

$$\begin{aligned} D_1 &= k_1^2, & D_2 &= (k_1+p_1)^2, \\ D_3 &= (k_1+p_{12})^2, & D_4 &= k_2^2, \\ D_5 &= (k_2+p_{12})^2, & D_6 &= (k_2+p_{123})^2, \\ D_7 &= (k_1-k_2)^2. \end{aligned} \tag{4.21}$$

We choose to start the loop-by-loop parametrisation with the k_2-loop, so that the only ISP we have to add is

$$D_8 = (k_1 + p_{123})^2. \tag{4.22}$$

As in the box-triangle diagram, the first step of the reduction consists in computing the Baikov polynomials [38], which are functions of the propagators ($D_i \to z_i$) and of the kinematic invariants (s, t).

We obtain

$$\begin{aligned}
\mathcal{E}_1 &= -\frac{s}{4}(z_1 z_3 + s z_8 - z_1 z_8 - z_3 z_8 + z_8^2), \\
\mathcal{B}_1 &= \frac{1}{16}\Big(z_3^2 z_4^2 - 2 z_1 z_3 z_4 z_5 + z_1^2 z_5^2 - 4 s z_1 z_3 z_6 + 2 s z_3 z_4 z_6 + 2 z_1 z_3 z_4 z_6 \\
&\quad - 2 z_3^2 z_4 z_6 + 2 s z_1 z_5 z_6 - 2 z_1^2 z_5 z_6 + 2 z_1 z_3 z_5 z_6 + s^2 z_6^2 - 2 s z_1 z_6^2 \\
&\quad + z_1^2 z_6^2 - 2 s z_3 z_6^2 - 2 z_1 z_3 z_6^2 + z_3^2 z_6^2 - 2 s z_3 z_4 z_7 - 2 s z_1 z_5 z_7 \\
&\quad - 2 s^2 z_6 z_7 + 2 s z_1 z_6 z_7 + 2 s z_3 z_6 z_7 + s^2 z_7^2 + 2 s z_3 z_4 z_8 - 2 z_3 z_4^2 z_8 \\
&\quad + 2 s z_1 z_5 z_8 - 4 s z_4 z_5 z_8 + 2 z_1 z_4 z_5 z_8 + 2 z_3 z_4 z_5 z_8 - 2 z_1 z_5^2 z_8 \\
&\quad - 2 s^2 z_6 z_8 + 2 s z_1 z_6 z_8 + 2 s z_3 z_6 z_8 + 2 s z_4 z_6 z_8 - 2 z_1 z_4 z_6 z_8 \\
&\quad + 2 z_3 z_4 z_6 z_8 + 2 s z_5 z_6 z_8 + 2 z_1 z_5 z_6 z_8 - 2 z_3 z_5 z_6 z_8 - 2 s^2 z_7 z_8 \\
&\quad + 2 s z_4 z_7 z_8 + 2 s z_5 z_7 z_8 - 4 s z_6 z_7 z_8 + s^2 z_8^2 - 2 s z_4 z_8^2 \\
&\quad + z_4^2 z_8^2 - 2 s z_5 z_8^2 - 2 z_4 z_5 z_8^2 + z_5^2 z_8^2 \Big), \\
\mathcal{E}_2 &= -\frac{1}{4} s t (s + t), \\
\mathcal{B}_2 &= \frac{1}{16}\Big(s^2 t^2 - 2 s t^2 z_1 + t^2 z_1^2 - 2 s^2 t z_2 + 2 s t z_1 z_2 + s^2 z_2^2 - 2 s t^2 z_3 \\
&\quad - 4 s t z_1 z_3 - 2 t^2 z_1 z_3 + 2 s t z_2 z_3 + t^2 z_3^2 - 2 s^2 t z_8 \\
&\quad + 2 s t z_1 z_8 - 2 s^2 z_2 z_8 - 4 s t z_2 z_8 + 2 s t z_3 z_8 + s^2 z_8^2 \Big).
\end{aligned} \tag{4.23}$$

It is evident that the polynomial expressions for the double-box is significantly more tangled than that of the box-triangle case, reflecting the higher structure complexity of the double-box configuration.

We proceed with the reduction following a similar procedure to the box-triangle case (cf. 4.2.1 and 4.2.2), in order to perform the reduction both in the no dimensional shift and no higher powers in the denominators cases. Analogously to the box-triangle case,

the reduction is implemented by accounting for the increased number of Baikov variables, which in this configuration is $n = 8$.

Furthermore, we identify the top sector of the family as

$$S_{\text{top}} = \{1, 1, 1, 1, 1, 1, 1, 0, 0\}. \tag{4.24}$$

The last two entries of eq. (4.24) correspond to the ISPs, in particular the last position represent the additional ISP required in the standard Baikov representation:

$$z_9 = (k_2 + p_1)^2. \tag{4.25}$$

However, had we performed the loop-by-loop parametrization starting from the k_1-loop, z_9 would have been the only ISP added, effectively ignoring z_8. We are now ready to perform the integral reductions for both cases comparing the results with the `FFIntRed` ones.

We choose to reduce all the integrals appearing in the IBPs with rank two and zero dots, we also fixed the seed integrals to have rank three and one dot. If we do not consider symmetries and mappings between the non-zero sectors of the family we obtain 30 MIs.

In any case, if we generate mapping identities between sectors and we add them to the IBP system solver, the number of MIs drops to a total number of 8, for both the no dimensional shift and no higher powers in the denominators cases, as expected from the Laporta reduction and from [52].

The MIs are

$$G_{\text{DBox}} = \begin{Bmatrix} \{1,1,1,1,1,1,1,-1,0\}, & \{1,1,1,1,1,1,1,0,0\}, & \{0,1,0,1,1,1,1,0,0\}, \\ \{0,1,1,1,0,1,1,0,0\}, & \{0,1,0,1,1,0,1,0,0\}, & \{1,0,1,1,1,0,0,0,0\}, \\ \{0,0,1,1,0,0,1,0,0\}, & \{0,1,0,0,0,1,1,0,0\} & \end{Bmatrix}. \tag{4.26}$$

We immediately notice that the top sector

$$I_{\text{top}} = \{1, 1, 1, 1, 1, 1, 1, 0, 0\} \tag{4.27}$$

is a master integral. All the corresponding graphs to MIs except for the top sector, are drawn in fig. 4.6.

In conclusion, the analysis performed in this chapter shows that the syzygy procedure significantly optimizes the reduction process by overcoming the traditional computational drawbacks. In other words, the integral reduction via a syzygy-based IBP generation within the loop-by-loop Baikov framework constitutes an effective alternative approach to the Laporta algorithm. Specifically, the implementation of syzygy constraints to suppress higher-order denominators allows us to bypass the computational bottlenecks typically encountered during the generation and solution of traditional IBP identities.

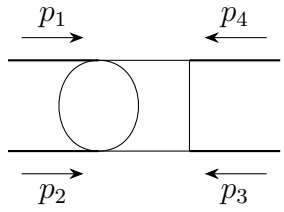

$G_3 = \{0, 1, 0, 1, 1, 1, 1, 0, 0\}$

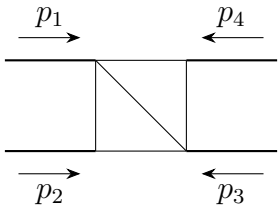

$G_4 = \{0, 1, 1, 1, 0, 1, 1, 0, 0\}$

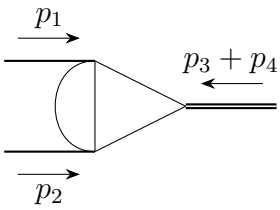

$G_5 = \{0, 1, 0, 1, 1, 0, 1, 0, 0\}$

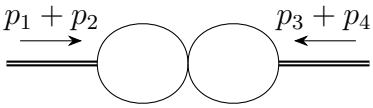

$G_6 = \{1, 0, 1, 1, 1, 0, 0, 0, 0\}$

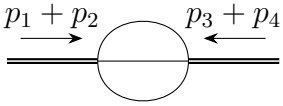

$G_7 = \{0, 0, 1, 1, 0, 0, 1, 0, 0\}$

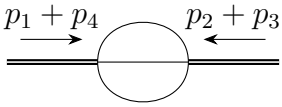

$G_8 = \{0, 1, 0, 0, 0, 1, 1, 0, 0\}$

Figure 4.6: Massless double-box family MIs and their corresponding configurations.

Chapter 5

Differential Equations via Polynomial Decomposition

In this chapter, we discuss an alternative method for deriving DEs for the MIs of a given family. As previously established (cf. Section 2.5), DEs provide a powerful framework to characterize the fundamental properties and analytic features of Feynman integral families.

Our objective is to derive these DEs by adopting the polynomial decomposition framework introduced in [44], adapting the procedure to our specific cases. Furthermore, the consistency of the outcomes is verified via the `FFIntRed` package, which yields a reliable environment for the derivation of DEs for MIs.

Specifically, the analysis focuses on the two families discussed in Chapter 4: the massless scalar box-triangle and the massless scalar double-box. Finally, in A we apply this method to derive DEs for a one loop case, namely the box family. This specific example is also treated from different persepective in [53], where the system of DEs is obtained without the needing of an integral reduction and avoiding higher powers in the propagators.

5.1 Differential Equations in Baikov Representation

In this section we discuss the procedure to follow in order to write DEs for FIs in loop-by-loop Baikov representation. Let us recall that, given an integral family, with MIs $\{G_j\}_{j=1}^{n_{\text{MIs}}}$ and a free parameter x the integrals depend on, we can reduce the derivative of the MIs with respect to x and write a system of DEs satisfied by $\{G_j\}$:

$$\partial_x G_j = \sum_{k \in \text{MIs}} A_{jk}^{(x)} G_k. \tag{5.1}$$

Since we work in the loop-by-loop Baikov representation, a generic integral has the following form

$$I_{\vec{a}} = K'' \int \mathrm{d}^n z \prod_{k=1}^{2L} \frac{\mathcal{B}_k^{\gamma_k}}{z_1^{a_1} \dots z_n^{a_n}}, \tag{5.2}$$

where we defined

$$K'' = \frac{\mathcal{J}(-i)^L \pi^{(L-n)/2}}{\prod_{l=1}^{L} \Gamma((D-E_l)/2)}. \tag{5.3}$$

Notice that, in the constant prefactor K'' we have not included the external polynomial $\mathcal{E}_L$, due to the fact that the external Baikov polynomial depends on the kinematic invariants. This term is essential since DEs are derived with respect to the parameter x, which can be identified with any such invariant.

Now, since the only term depending on x in the integrand is $\mathcal{B}_k$, we can write

$$\partial_x I_{\vec{a}} = \int \mathrm{d}^n z \sum_{k=1}^{2L} \frac{\gamma_k}{\mathcal{B}_k} (\partial_x \mathcal{B}_k) \frac{\mathcal{B}_k^{\gamma_k}}{z_1^{a_1} \dots z_n^{a_n}}, \tag{5.4}$$

where we dropped the constant prefactor K' to simplify the notation.

Moreover, we can arbitrarily add or subtract from this equation the total derivative in eq. (4.2):

$$\partial_x I_{\vec{a}} = \int \mathrm{d}^n z \sum_{k=1}^{2L} \frac{\gamma_k}{\mathcal{B}_k} (\partial_x \mathcal{B}_k) \frac{\mathcal{B}_k^{\gamma_k}}{z_1^{a_1} \dots z_n^{a_n}} - \sum_{i=1}^{n} \int \mathrm{d}^n z \frac{\partial}{\partial z_i} \left(g_i \prod_{k=1}^{2L} \frac{\mathcal{B}_k^{\gamma_k}}{z_1^{a_1} \dots z_n^{a_n}} \right), \tag{5.5}$$

for some suitable polynomials $g_i(\mathbf{z}, x)$. If we apply Leibniz rule to the total derivative, we obtain

$$\partial_x I_{\vec{a}} = \sum_{k=1}^{2L} \int \mathrm{d}^n z \frac{\gamma_k}{\mathcal{B}_k} (\partial_x \mathcal{B}_k) \frac{\mathcal{B}_k^{\gamma_k}}{z_1^{a_1} \dots z_n^{a_n}} - \sum_{i=1}^{n} \sum_{k=1}^{2L} \int \mathrm{d}^n z \left(\frac{\partial g_i}{\partial z_i} + \frac{\gamma_k}{\mathcal{B}_k} g_i \frac{\partial \mathcal{B}_k}{\partial z_i} - a_i \frac{g_i}{z_i} \right) \frac{\prod_{m \neq k} \mathcal{B}_m^{\gamma_m}}{z_1^{a_1} \dots z_n^{a_n}}. \tag{5.6}$$

The structure of the expression above is closely related to the IBP identities in the loop-by-loop Baikov representation in eq. (4.5). However, it presents an additional contribution—the first term on the right-hand side—arising from the explicit dependence of the Baikov polynomials on the kinematic parameter x.

Furthermore, we can write an equation which has a form similar to syzygy equations, except that it has a non vanishing right-hand side, namely a *polynomial decomposition* equation:

$$\vec{f}(\mathbf{z}) \cdot \vec{g}(\mathbf{z}) = h(\mathbf{z}), \tag{5.7}$$

where $f(\mathbf{z})$ and $g(\mathbf{z})$ are lists of known and unknown polynomials respectively and $h(\mathbf{z})$ is also a known polynomial. Hence, defining $B \equiv \prod_{k=1}^{2L} \mathcal{B}_k$, we can write

$$h_0 B = \sum_{k=1}^{2L} \left[\gamma_k (\partial_x \mathcal{B}_k) - \sum_{i=1}^{n} g_i \gamma_k \frac{\partial \mathcal{B}_k}{\partial z_i} \right] \prod_{j \neq k} \mathcal{B}_j. \tag{5.8}$$

In particular, we can identify

$$\begin{cases} \vec{f}(\mathbf{z}) = \left\{ B, \sum_{k=1}^{2L} \gamma_k \frac{\partial \mathcal{B}_k}{\partial z_1} \prod_{j \neq k} \mathcal{B}_j, \ldots, \sum_{k=1}^{2L} \gamma_k \frac{\partial \mathcal{B}_k}{\partial z_n} \prod_{j \neq k} \mathcal{B}_j \right\}, \\ \vec{g}(\mathbf{z}) = \{ g_1, \ldots, g_n, h_0 \}, \\ h(\mathbf{z}) = \sum_{k=1}^{2L} \gamma_k (\partial_x \mathcal{B}_k) \prod_{j \neq k} \mathcal{B}_j. \end{cases} \tag{5.9}$$

If we plug the equation above in eq. (5.6) we obtain the master formula

$$\partial_x I_{\vec{a}} = \int \mathrm{d}^n z \sum_{i=1}^{n} \left[-\frac{\partial g_i}{\partial z_i} + a_i \frac{g_i}{z_i} + h_0 \right] \frac{\prod_{k=1}^{2L} \mathcal{B}_k^{\gamma_k}}{z_1^{a_1} \ldots z_n^{a_n}}. \tag{5.10}$$

Alternatively, in order to avoid that the right-handed side generates higher powers in the denominators, we can rewrite the equation above using the syzygy solution (4.4), obtaining

$$\partial_x I_{\vec{a}} = \int \mathrm{d}^n z \sum_{i=1}^{n} \left[-\frac{\partial (h_i z_i)}{\partial z_i} + a_i h_i + h_0 \right] \frac{\prod_{k=1}^{2L} \mathcal{B}_k^{\gamma_k}}{z_1^{a_1} \ldots z_n^{a_n}}. \tag{5.11}$$

In summary, this section has demonstrated how the derivation of DEs for FIs can be implemented through a polynomial decomposition-based approach. This framework allows for the explicit construction of the differential system—regardless of whether the parameter x represents a particle mass or a Mandelstam invariant—leading to the systematic reconstruction of the matrix $A_{jk}^{(x)}$ in eq. (5.1).

5.2 The Box-Triangle Case

In this section we discuss the derivation of the system of DEs for the box-triangle family showed in fig. 4.1. Since we are considering the massless case, with three external momenta, the only kinematic variable with respect to which we can differentiate our integrals is the Mandelstam invariant

$$\frac{s}{2} = p_1 \cdot p_2. \tag{5.12}$$

Notice that, since the box-triangle family depends only on one energy scale, deriving the DEs is quite trivial. In fact, we can rewrite a generic integral belonging to the family, highlighting the s-dependence as

$$I_{\vec{a}} \sim s^N. \tag{5.13}$$

Hence,

$$\partial_s I_{\vec{a}} = \frac{N}{s} I_{\vec{a}}. \tag{5.14}$$

Since we know from the integral reduction performed in Chapter 4 that the MIs are

$$G_{\text{TBox}} = \{G_k\}_{k=1}^3 = \{\{1,1,1,0,1,0,0\},\{0,1,1,1,0,0,0\},\{0,1,0,1,1,1,0\}\}, \tag{5.15}$$

we expect to obtain a system of the form

$$\partial_s G_{\text{TBox}} = \begin{pmatrix} \frac{N_1}{s} & 0 & 0 \\ 0 & \frac{N_2}{s} & 0 \\ 0 & 0 & \frac{N_3}{s} \end{pmatrix} \begin{pmatrix} G_1 \\ G_2 \\ G_3 \end{pmatrix}, \tag{5.16}$$

where N_i is the dimensional coefficient for the i-th master integral G_i. Note that the matrix in the system of DEs is diagonal, due to eq. (5.14). We could compute directly the coefficients N_i via dimensional analysis. In particular, the mass dimension N_i is given by

$$N_i \equiv [G_i] = n + \sum_{k=1}^{2L} \gamma_k [\mathcal{B}_k] - \sum_{i=1}^{n_{\text{active}}} a_i. \tag{5.17}$$

Now, in order to write the DEs via a polynomial decomposition, we employ the `CALICO` function `CATPolyDec` [44]:

$$g = \texttt{CATPolyDec}[\{f_1(\mathbf{z}),\ldots,f_k(\mathbf{z})\},\{h_1(\mathbf{z}),\ldots,h_m(\mathbf{z})\},d_{\max}], \tag{5.18}$$

which returns a m-dimensional list, whose i-th entry is a solution of eq. (5.7) for $h(\mathbf{z}) = h_i(\mathbf{z})$.

In our case, according to eq. (5.9), we have $m = 1$. We find the following solutions

$$\begin{aligned} g_i &= -\frac{z_i}{s}, \quad \forall i = 1,\ldots,6 \\ h_0 &= -\frac{6+D}{s}, \end{aligned} \tag{5.19}$$

where $D = 4-2\epsilon$. We implement eq. (5.10) and apply it to each master integral. Firstly, we obtain DEs of the form

$$\partial_s G_j = \sum_{k=1}^{3} h_{jk}^{(s)} I_k, \tag{5.20}$$

where the equations are expressed in terms of unreduced integrals I_k. By performing the reduction via the syzygy approach presented in Chapter 4, we obtain the following system of DEs:

$$\partial_s G_{\text{TBox}} = \begin{pmatrix} -\frac{2\epsilon}{s} & 0 & 0 \\ 0 & -\frac{2\epsilon}{s} & 0 \\ 0 & 0 & \frac{1-2\epsilon}{s} \end{pmatrix} \begin{pmatrix} G_1 \\ G_2 \\ G_3 \end{pmatrix}. \tag{5.21}$$

We observe that the DEs for the massless box-triangle family, completely decouple, since the matrix $A^{(s)}$ takes a diagonal form, reflecting the lesser complexity of the family.

Furthermore, we perform the same computation but in the case of suppression of higher powers in the denominators of the unreduced integrals I_k, by considering the syzygy solutions (4.4). Hence,

$$g_i \to h_i = \frac{g_i}{z_i} = -\frac{1}{s}, \tag{5.22}$$

leads identically to the same result, confirming the consistency of the reduction scheme.

Finally, we verify the consistency of the result by generating and reducing the derivatives of the MIs via `FFIntRed`, yielding the expected outcome (5.21). Furthermore, we observe that the number of integrals requiring reduction within the DEs depends significantly on the chosen reduction strategy. As summarized in tab. 5.1, using the decomposition constraint without dimensional shift results in a slightly larger set of unreduced integrals compared to the `FFIntRed` ones. Furthermore, if we also exclude from the start integrals without higher power in the denominators , the system of DEs is already reduced.

Method	**Number of unreduced FIs in the derivatives**
`FFIntRed` (Standard differentiation)	7
PD + No Dimension Shift	9
PD + No Higher Powers	0

Table 5.1: Number of unreduced FIs generated during the derivation of the DEs for the box-triangle family. We compare standard differentiation with polynomial decomposition (PD) methods.

5.3 The Double-Box Case

In this section we present the derivation of the system of DEs for the massless double-box family as in fig. 4.5. In this case, the analysis involves two distinct systems of equations, corresponding to the two independent Mandelstam invariants that characterize the kinematics of the process

$$\frac{s}{2} = p_1 \cdot p_2, \quad \frac{t}{2} = p_2 \cdot p_3. \tag{5.23}$$

We follow the same procedure of the previous case, which can be summarized as:

- Identify the MIs of the family.
- Reconstruct the solutions $\{g_i, h_0\}$ of the polynomial decomposition.
- Implement the system of DEs in eq. (5.10) and reduce the obtained integrals.
- Reconstruct the matrix $A^{(x)}_{jk}$ and verify its consistency with `FFIntRed`.
- Repeat the calculation for the set of solutions $\{h_i, h_0\}$, in order to avoid higher powers in the propagators of the unreduced derivatives.

Following this prescription, we proceed to derive the DEs for the double-box family with respect to both kinematic invariants s and t.

Let us recall the MIs expressions for the double-box family

$$G_{\text{DBox}} = \begin{Bmatrix} \{1,1,1,1,1,1,1,-1,0\}, & \{1,1,1,1,1,1,1,0,0\}, & \{0,1,0,1,1,1,1,0,0\}, \\ \{0,1,1,1,0,1,1,0,0\}, & \{0,1,0,1,1,0,1,0,0\}, & \{1,0,1,1,1,0,0,0,0\}, \\ \{0,0,1,1,0,0,1,0,0\}, & \{0,1,0,0,0,1,1,0,0\} & \end{Bmatrix}. \tag{5.24}$$

After reconstructing the solutions $\{g_i, h_0\}$ and reducing the system of DEs with respect to s and t we obtain the following matrices:

$$A^{(s)} = \begin{pmatrix} -\frac{2(1+\epsilon)}{s} - \frac{\epsilon}{s+t} & \frac{\epsilon t}{s+t} & \frac{12A}{s(s+t)} & -\frac{18\epsilon}{s^2} & \frac{15B}{2\epsilon s^2(s+t)} & \frac{A^2(s+2t)}{\epsilon s^3(s+t)} & \frac{6A(9\epsilon^2-9\epsilon+2)}{\epsilon^2 s^3(s+t)} & \frac{9C}{\epsilon^2 s^2 t(s+t)} \\ \frac{2\epsilon}{s(s+t)} & -\frac{2(s+t+\epsilon t)}{s(s+t)} & \frac{12A}{st(s+t)} & -\frac{12\epsilon}{s^2 t} & \frac{3B(2s+t)}{\epsilon s^3 t(s+t)} & \frac{2A^2}{\epsilon s^3(s+t)} & \frac{6C(s-t)}{\epsilon^2 s^4 t(s+t)} & \frac{6C}{\epsilon^2 s^2 t^2(s+t)} \\ 0 & 0 & -\frac{s+t+\epsilon t}{s(s+t)} & 0 & \frac{3\epsilon-1}{s(s+t)} & 0 & 0 & \frac{9\epsilon^2-9\epsilon+2}{\epsilon st(s+t)} \\ 0 & 0 & 0 & -\frac{s+2\epsilon t}{s(s+t)} & 0 & 0 & \frac{2+\epsilon(-13+9\epsilon(3-2\epsilon))}{\epsilon^2 s^2(s+t)} & \frac{C}{\epsilon^2 st(s+t)} \\ 0 & 0 & 0 & 0 & -\frac{2\epsilon}{s} & 0 & 0 & 0 \\ 0 & 0 & 0 & 0 & 0 & -\frac{2\epsilon}{s} & 0 & 0 \\ 0 & 0 & 0 & 0 & 0 & 0 & -\frac{A}{s} & 0 \\ 0 & 0 & 0 & 0 & 0 & 0 & 0 & 0 \end{pmatrix}, \tag{5.25}$$

where we introduced the following polynomial factors:

$$\begin{aligned} A &= A(\epsilon) \equiv 2\epsilon - 1, \\ B &= B(\epsilon) \equiv 1 + \epsilon(6\epsilon - 5), \\ C &= C(\epsilon) \equiv A(\epsilon)(3\epsilon - 2)(3\epsilon - 1). \end{aligned} \tag{5.26}$$

In contrast to the previous case, the presence of off-diagonal entries signals that the system of DEs is coupled. The first two rows, which correspond to the top sector, are consistent with the hierarchical structure of FIs: as the highest sectors in the family, their derivatives naturally depend on the MIs of the lower sectors. Accordingly, the matrix is predominantly upper triangular, reflecting the fact that lower integrals do not receive contributions from higher sectors.

Regarding the t-matrix, we obtain

$$A^{(t)} = \begin{pmatrix} \frac{\epsilon s}{t(s+t)} & -\frac{\epsilon s}{s+t} & -\frac{12A}{t(s+t)} & \frac{18\epsilon}{st} & -\frac{15B}{2\epsilon st(s+t)} & -\frac{A^2(s+2t)}{\epsilon s^2 t(s+t)} & -\frac{6A(9\epsilon^2-9\epsilon+2)}{\epsilon^2 s^2 t(s+t)} & -\frac{9C}{\epsilon^2 st^2(s+t)} \\ -\frac{2\epsilon}{t(s+t)} & -\frac{s+t+2\epsilon s}{t(s+t)} & -\frac{12A}{t^2(s+t)} & \frac{12\epsilon}{st^2} & -\frac{3B(2s+t)}{\epsilon s^2 t^2(s+t)} & -\frac{2A^2}{\epsilon s^2 t(s+t)} & -\frac{6C(s-t)}{\epsilon^2 s^3 t^2(s+t)} & \frac{6(2+\epsilon(-13+9\epsilon(3-2\epsilon)))}{\epsilon^2 st^3(s+t)} \\ 0 & 0 & \epsilon\left(\frac{1}{s+t}-\frac{2}{t}\right) & 0 & \frac{1-3\epsilon}{t(s+t)} & 0 & 0 & -\frac{9\epsilon^2-9\epsilon+2}{\epsilon t^2(s+t)} \\ 0 & 0 & 0 & -\frac{2\epsilon s+t}{t(s+t)} & 0 & 0 & \frac{C}{\epsilon^2 st(s+t)} & \frac{2+\epsilon(-13+9\epsilon(3-2\epsilon))}{\epsilon^2 t^2(s+t)} \\ 0 & 0 & 0 & 0 & 0 & 0 & 0 & 0 \\ 0 & 0 & 0 & 0 & 0 & 0 & 0 & 0 \\ 0 & 0 & 0 & 0 & 0 & 0 & 0 & 0 \\ 0 & 0 & 0 & 0 & 0 & 0 & 0 & -\frac{A}{t} \end{pmatrix}. \tag{5.27}$$

The matrix $A^{(t)}$ exhibits a structure consistent with the previous findings. Note that, the null entries in rows 5, 6, and 7 indicate that the corresponding MIs are independent of the t-channel kinematics, a feature expected from the topology of the massless double-box family.

To ensure the mathematical consistency of the entire system, we verified that the two matrices satisfy the integrability condition (2.51):

$$\partial_t A^{(s)} - \partial_s A^{(t)} + [A^{(s)}, A^{(t)}] = 0. \tag{5.28}$$

Finally, we verified the consistency of our calculation via `FFIntRed`, considering also the avoidance of higher powers denominators case. The outcomes of this computation match perfectly the results in eqs. (5.25) and (5.27). Thus, deriving DEs systems for the MIs of a given integral family in the loop-by-loop Baikov representation via a polynomial decomposion-based approach represents a valid and successfull alternative method to study FIs properties.

In conclusion, tab. 5.2 summarizes the number of unreduced integrals for each approach. Similar to the box-triangle family, we observe a consistent pattern: when integrals with higher-power propagators are excluded, deriving the system of DEs via

polynomial decomposition is more efficient than the standard Laporta-based reduction, as it results in a smaller set of unreduced integrals.

Method	**Number of unreduced FIs in the derivatives**
`FFIntRed` (standard differentiation)	41
PD + No Dimension Shift	45
PD + No Higher Powers	32

Table 5.2: Number of unreduced FIs generated during the derivation of the DEs for the double-box family. We compare standard differentiation with polynomial decomposition (PD) methods.

Chapter 6

Conclusions

In this thesis, we have presented and implemented a syzygy-based approach for the reduction of Feynman integral families within the loop-by-loop Baikov representation. After establishing the theoretical foundations in the Feynman parametric representation, discussing the concept of MIs, the derivation of IBP identities, and the construction of DEs in canonical form, we specialized this formalism to modern multi-loop calculation requirements.

We provided a detailed analysis of the Baikov representation, comparing the standard and loop-by-loop parametrisations. By employing the theory of syzygy equations, we adapted the IBP generation to the loop-by-loop framework, significantly reducing the algebraic complexity typically associated with multi-loop topologies. The validity of this formalism was demonstrated through two-loop case studies: the massless box-triangle and the massless double-box families. The reduction was implemented in a `Mathematica` environment using the `FiniteFlow` framework, and its accuracy was verified against the `FFIntRed` package.

A key finding of this work is the algorithm built in the loop-by-loop Baikov representation, combined with syzygy equations, to generate IBP identities that prevent the appearance of increased propagator powers, thus optimizing the reduction process.

Furthermore, we extended this approach to the derivation of the DEs system for the MIs of using polynomial decomposition techniques. The successful verification of these results with `FFIntRed` confirms that the combination of the loop-by-loop Baikov representation and syzygy-based reductions provides an efficient alternative to traditional Laporta algorithms.

In conclusion, the methodology presented in this thesis offers a general algorithm for the systematic analysis of the properties of multi-loop integral families in quantum field theory.

A

Differential Equations of the Box Family

In this appendix we review the derivation of the system of DEs for the one-loop massless scalar box family, based on the treatment provided by [19, 30]. The box family is depicted in fig. A.1, with four external momenta $p_i, i = 1, 2, 3, 4$ and loop momentum k. We also write the system in canonical form and find the solutions of the DEs.

The box family is defined as

$$I^{\text{box}}_{a_1,a_2,a_3,a_4} = \int \frac{\mathrm{d}^D k}{i\pi^{D/2}} \frac{1}{D_1^{a_1} D_2^{a_2} D_3^{a_3} D_4^{a_4}}, \tag{A.1}$$

where the propagators are defined as

$$\begin{aligned} D_1 &= k^2, & D_2 &= (k + p_1)^2, \\ D_3 &= (k + p_1 + p_2)^2, & D_4 &= (k - p_4)^2. \end{aligned} \tag{A.2}$$

Moreover, due to momentum conservation, $p_1 + p_2 + p_3 + p_4 = 0$. We can define also the Mandlestam invariants for the family as

$$s = 2p_1 \cdot p_2, \quad t = 2p_1 \cdot p_4. \tag{A.3}$$

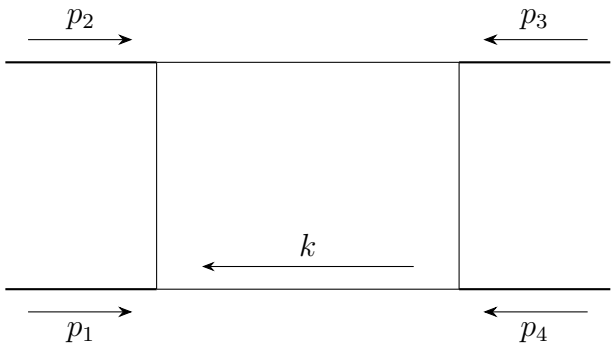

Figure A.1: One loop box integral family, with loop momentum k.

Our starting point in the analysis consists in finding the MIs of the family, using the syzygy-based method presented in Chapter 4. Alternatively, one could perform the reduction via Laporta algorithm.

The reduction yields three MIs, represented in fig. A.2:

$$\vec{g}(s,t;\epsilon) = \begin{pmatrix} I_{0,1,0,1} \\ I_{1,0,1,0} \\ I_{1,1,1,1} \end{pmatrix}. \tag{A.4}$$

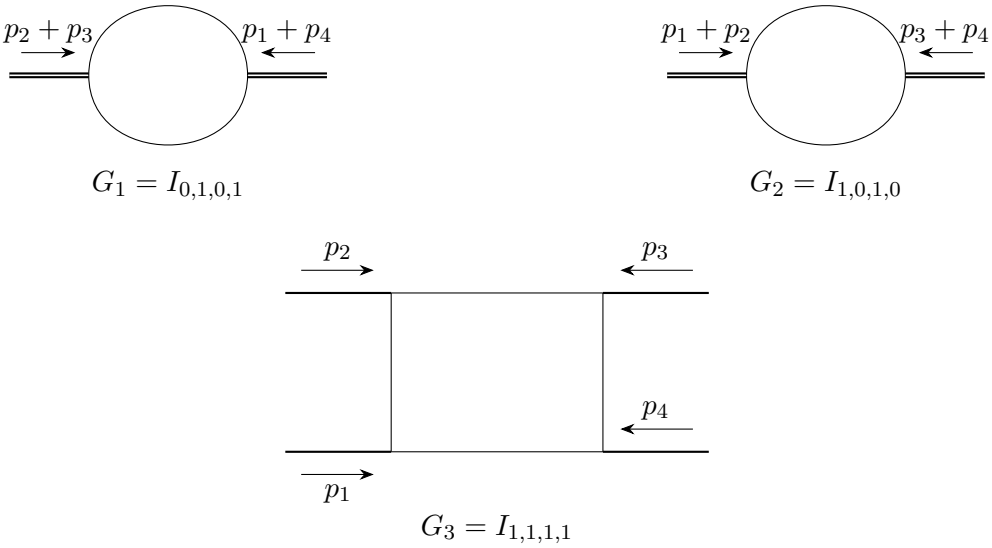

Figure A.2: Box family MIs and their corresponding configurations.

Now, using the polynomial decomposition approached developed in Chapter 5, we derive the system of DEs for our set of MIs:

$$\begin{cases} \partial_s \vec{g}(s,t;\epsilon) = A^{(s)} \vec{g}(s,t;\epsilon), \\ \partial_t \vec{g}(s,t;\epsilon) = A^{(t)} \vec{g}(s,t;\epsilon). \end{cases} \tag{A.5}$$

In particular, we find the following expression for the matrices $A^{(s)}, A^{(t)}$:

$$A^{(s)} = \begin{pmatrix} 0 & 0 & 0 \\ 0 & -\frac{\epsilon}{s} & 0 \\ \frac{2(-1+2\epsilon)}{st(s+t)} & -\frac{2(-1+2\epsilon)}{s^2(s+t)} & -\frac{s+t+\epsilon t}{s(s+t)} \end{pmatrix}, \quad A^{(t)} = \begin{pmatrix} -\frac{\epsilon}{t} & 0 & 0 \\ 0 & 0 & 0 \\ -\frac{2(-1+2\epsilon)}{t^2(s+t)} & \frac{2(-1+2\epsilon)}{st(s+t)} & -\frac{s+\epsilon s+t}{t(s+t)} \end{pmatrix}. \tag{A.6}$$

Furthermore, $A^{(s)}$ and $A^{(t)}$ satisfy the integrability condition

$$\partial_t A^{(s)} - \partial_s A^{(t)} + [A^{(s)}, A^{(t)}] = 0. \tag{A.7}$$

Now, in order to write the system of DEs in canonical form we have to perform a change of basis:

$$\vec{f}(s,t;\epsilon) = c(\epsilon) \begin{pmatrix} tI_{0,1,0,2} \\ sI_{1,0,2,0} \\ \epsilon st I_{1,1,1,1} \end{pmatrix}, \tag{A.8}$$

where $c(\epsilon) = \epsilon e^{\gamma_E}$ is a normalization factor, with γ_E being the Euler-Mascheroni constant. Moreover, we express the basis transformation as

$$\vec{f} = T^{-1} \vec{g}, \tag{A.9}$$

where

$$T^{-1} = \begin{pmatrix} 0 & 0 & \epsilon st \\ 0 & 2\epsilon - 1 & 0 \\ 2\epsilon - 1 & 0 & 0 \end{pmatrix} \tag{A.10}$$

is obtained by reducing the integrals in eq. (A.8). Thus, in the new basis, the system is in ϵ-form:

$$\begin{cases} \partial_s \vec{f}(s,t;\epsilon) = \epsilon B^{(s)} \vec{f}(s,t;\epsilon) \\ \partial_t \vec{f}(s,t,\epsilon) = \epsilon B^{(t)} \vec{f}(s,t;\epsilon). \end{cases} \tag{A.11}$$

In particular, we compute $B^{(s)}$ and $B^{(t)}$ by using eq. (2.68), yielding

$$B^{(s)} = \begin{pmatrix} -\frac{t}{s(s+t)} & -\frac{2t}{s(s+t)} & \frac{2}{s+t} \\ 0 & -\frac{1}{s} & 0 \\ 0 & 0 & 0 \end{pmatrix}, \quad B^{(t)} = \begin{pmatrix} -\frac{s}{t(s+t)} & \frac{2}{s+t} & -\frac{2s}{t(s+t)} \\ 0 & 0 & 0 \\ 0 & 0 & -\frac{1}{t} \end{pmatrix}, \tag{A.12}$$

noting that the alphabet of this family is composed of three letters $\{s, t, s+t\}$.

Furthermore, let us perform a change of variable $t \equiv sx$, thus

$$\begin{aligned} B^{(s)} \to C^{(s)} &= B^{(s)} + \frac{t}{s} B^{(t)}\Big|_{t=sx}, \\ B^{(t)} \to C^{(x)} &= s B^{(t)}\Big|_{t=sx}. \end{aligned} \tag{A.13}$$

Explicitly we obtain

$$C^{(s)} = \begin{pmatrix} -\frac{1}{s} & 0 & 0 \\ 0 & -\frac{1}{s} & 0 \\ 0 & 0 & -\frac{1}{s} \end{pmatrix}, \quad C^{(x)} = \begin{pmatrix} -\frac{1}{x(1+x)} & \frac{2}{1+x} & -\frac{2}{x(1+x)} \\ 0 & 0 & 0 \\ 0 & 0 & -\frac{1}{x} \end{pmatrix}. \tag{A.14}$$

Thus, we can rewrite the canonical form of the system following eq. (2.80):

$$\mathrm{d}\,\vec{f}(s,x;\epsilon) = [\mathrm{d}\,\tilde{A}(s,x)]\vec{f}(s,x;\epsilon). \tag{A.15}$$

In particular, we can express $\mathrm{d}\,\tilde{A}$ using eq. (2.81) where

$$\{\alpha_k\}_{k=1}^{3} = \{s, x, 1+x\}. \tag{A.16}$$

Moreover, we extract the matrix coefficients A_k by eq. (A.14):

$$A_1 = \begin{pmatrix} -1 & 0 & 0 \\ 0 & -1 & 0 \\ 0 & 0 & -1 \end{pmatrix}, \quad A_2 = \begin{pmatrix} -1 & 0 & -2 \\ 0 & 0 & 0 \\ 0 & 0 & -1 \end{pmatrix}, \quad A_3 = \begin{pmatrix} 1 & 2 & 2 \\ 0 & 0 & 0 \\ 0 & 0 & 0 \end{pmatrix}. \tag{A.17}$$

Now, we compute the analytic solution of the system by factorizing the s-dependence using dimensional analysis:

$$\vec{f}(s,x;\epsilon) = (-s)^{-\epsilon}\vec{h}(x;\epsilon). \tag{A.18}$$

Moreover, we write the recursive relation

$$\partial_x \vec{h}^{(k)}(x) = \left[\frac{A_2}{x} + \frac{A_3}{1+x}\right]\vec{h}^{(k-1)}(x), \tag{A.19}$$

which can be solved order by order by using eq. (2.63).

Since $h_2(x,\epsilon)$ and $h_3(x,\epsilon)$ are bubble integrals, we can expand the result obtained in eq. (2.29) around $\epsilon = 0$ up to order 3, yielding

$$\begin{aligned} h_2(x;\epsilon) &= -1 + \epsilon^2\frac{\pi^2}{12} + \epsilon^3\frac{7}{3}\zeta_3 + \mathcal{O}(\epsilon^4), \\ h_3(x;\epsilon) &= -1 + \epsilon\log(x) + \frac{\epsilon^2}{12}[\pi^2 - 6\log^2(x)] + \frac{\epsilon^3}{12}[2\log^3(x) - \pi^2\log(x) + 28\zeta_3] + \mathcal{O}(\epsilon^4), \end{aligned} \tag{A.20}$$

where ζ_s is the Riemann zeta function defined as

$$\zeta_s = \sum_{n=1}^{\infty} \frac{1}{n^s}. \tag{A.21}$$

Finally, we note that the integral $I_{1,1,1,1}$ does not admit a u-channel, thus $h_1(x;\epsilon)$ must be finite in the limit $x \to -1$. This condition fixes the solution to all orders in ϵ, yielding

$$\begin{aligned} h_1(x;\epsilon) =& 4 + \epsilon\Big[-2\log x\Big] + \epsilon^2\left[-\frac{4\pi^2}{3}\right] \\ &+ \epsilon^3\left[\frac{7\pi^2}{6}\log x + \frac{1}{3}\log^3 x - \pi^2\log(1+x) - \log^2 x \log(1+x)\right. \\ &\left. - 2\log x\,\mathrm{Li}_2(-x) + 2\,\mathrm{Li}_3(-x) - \frac{34}{3}\zeta_3\right] + \mathcal{O}(\epsilon^4). \end{aligned} \tag{A.22}$$

B

Derivation of the Baikov Representation

In this appendix we review a detailed derivation of the Baikov representation, a fundamental framework utilized throughout this work for the reduction of multi-loop FIs. While the main text focuses on the application of this representation to specific topologies, we collect here the explicit calculations and geometrical considerations required to map loop-momenta integrals into the space of Baikov variables. We follow the derivation provided by [38].

B.1 The One Loop Case

Let us consider a Feynman integral in momentum representation, as in eq. (2.12). Since we are focusing on the one-loop case, we have

$$I = \int \frac{\mathrm{d}^D k}{i\pi^{D/2}} \frac{1}{D_1^{a_1} \dots D_{E+1}^{a_{E+1}}}, \tag{B.1}$$

where E is the number of independent external momenta of the diagram.

Firstly, we separate the integration region into a parallel and a transverse component with respect to the external momenta $\{p_1, \dots p_E\}$, i.e.

$$k = k_\parallel + k_\perp, \quad k_\parallel \cdot k_\perp = 0. \tag{B.2}$$

Thus, the integration becomes

$$\mathrm{d}^D k = \mathrm{d}^E k_\parallel \, \mathrm{d}^{D-E} k_\perp. \tag{B.3}$$

We can perform a change of coordinates on the part of the integrand depending on $k_\perp$, splitting it in a radial and an angular part: $\mathrm{d}^{D-E} k_\perp = k_\perp^{D-E-1} \, \mathrm{d} k_\perp \, \mathrm{d} \Omega_{D-E-1}$, yielding

$$I = \frac{1}{i\pi^{D/2}} \int \frac{|k_\perp|^{D-E-1} \,\mathrm{d}^E\, k_\parallel \,\mathrm{d}\,|k_\perp| \,\mathrm{d}\,\Omega_{D-E-1}}{D_1^{a_1} \dots D_{E+1}^{a_{E+1}}}. \tag{B.4}$$

The angular spherical integral is performed using

$$\int \mathrm{d}\,\Omega_n = \frac{2\pi^{\frac{n}{2}}}{\Gamma(\frac{n}{2})}. \tag{B.5}$$

Thus we can write, combining with result with the additional change of variable $k_\perp \to k_\perp^2$:

$$I = \frac{1}{\Gamma(\frac{D-E}{2}) i\pi^{E/2}} \int \frac{(k_\perp^2)^{\frac{D-E-2}{2}} \,\mathrm{d}^E\, k_\parallel \,\mathrm{d}(k_\perp)^2}{D_1^{a_1} \dots D_{E+1}^{a_{E+1}}}. \tag{B.6}$$

Now, we aim to rewrite the integration over $k_\parallel$ in a convenient way, by introducing the variables $\xi_i \equiv k \cdot p_i = k_\parallel \cdot p_i$. It is easy to realise that

$$\mathrm{d}^E\, \xi = \det({p_i}^j) \,\mathrm{d}^E\, k_\parallel, \tag{B.7}$$

where $\mathrm{d}\,\xi_i / \mathrm{d}\, k_\parallel^j = {p_i}^j$. In particular, the matrix ${p_i}^j$ is related to the Gram matrix $G(p_1, \dots, p_E)$ and its determinant $\mathcal{E}$, in fact:

$$\mathrm{d}^E\, k_\parallel = \mathcal{E}^{-\frac{1}{2}} \,\mathrm{d}\,\xi_1 \dots \mathrm{d}\,\xi_E, \tag{B.8}$$

thus we can naturally identify

$$\mathcal{E} = \det[G(p_1, \dots, p_E)] \tag{B.9}$$

with the external Baikov polynomial.

Regarding the integration over $(k_\perp)^2$, we introduce the variable $\xi_0 \equiv k^2 = k_\parallel^2 + k_\perp^2$, thus $\mathrm{d}\,\xi_0 / \mathrm{d}\, k_\perp^2 = 1$ and

$$\mathrm{d}^E\, k_\parallel \times \mathrm{d}(k_\perp)^2 = \mathrm{d}^E\, k_\parallel \times \mathrm{d}\,\xi_0. \tag{B.10}$$

Now, in order to obtain the Baikov polynomial

$$\mathcal{B} = \det[G(k, p_1, \dots, p_E)], \tag{B.11}$$

we rewrite $k = k_\perp + k_\parallel = k_\perp + \sum_{i=1}^E \kappa_i p_i$, where κ_i is the component of the externl momentum p_i along $k_\parallel$. Therefore, since determinants are invariant under shifting of rows/columns with multiples of rows/columns, we observe that a Gram determinant is invariant under shifting of the momenta within its vector space.

Thus we can redefine

$$\mathcal{B} = \det[G(k_\perp, p_1, \dots, p_E)] \tag{B.12}$$

and compute, using the result in [41]:

$$\mathcal{B} = (k_\perp)^2 \det[G(p_1, \ldots, p_E)] = (k_\perp)^2 \mathcal{E}. \tag{B.13}$$

Now, inserting eqs. (B.8), (B.10), (B.12) in the integral, we obtain

$$I_{\text{one-loop}} = \frac{-i\pi^{-E/2}\mathcal{E}^{\frac{E-D+1}{2}}}{\Gamma(\frac{D-E}{2})} \int_{\mathcal{C}} \frac{\mathcal{B}^{\frac{D-E-2}{2}}\, \mathrm{d}^{E+1}\xi}{D_1^{a_1} \ldots D_{E+1}^{a_{E+1}}}. \tag{B.14}$$

In particular, the requirement $k_\perp^2 > 0$ is interpreted as the definition of the integration region $\mathcal{C}$ in eq. (3.7).

Finally, performing the final change of variable $\xi_i \to z_i = D_i$, we obtain the one-loop Baikov representation in eq. (3.9).

B.2 The Loop-by-Loop Baikov Case

In the L-loops case a Feynman integral in momentum representation appears as in eq. (2.19). In order to derive the loop-by-loop parametrisation, we can follow the same steps of the one-loop case, taking into account that we have to replace $E \to E_i, \mathcal{B} \to \mathcal{B}_i$ and $\mathcal{E} \to \mathcal{E}_i$, , with $i = 1, \ldots, L$. Thus, the polynomials $\mathcal{E}_i$ now must not be taken out of the integration carelessly, since they could depend on the loop momenta of the remaining loops.

Furthermore, as discussed in Chapter 3, the number of integration variables does not match in general the number of propagators in the loop-by-loop case, we have to consider also the irreducible scalar products (ISPs).

Thus we can write

$$I_{\text{lbl}} = \frac{(-i)^L \pi^{\frac{L-n}{2}}}{\prod_{l=1}^{L} \Gamma(\frac{D-E_l}{2})} \int_{\mathcal{C}} \frac{\prod_{l=1}^{L} \mathcal{E}_l^{(E_l-D+1)/2} \mathcal{B}_l^{(D-E_l-2)/2}}{D_1^{a_1} \ldots D_n^{a_n}}\, \mathrm{d}^n \xi, \tag{B.15}$$

where

$$n = \sum_{l=1}^{L} (E_l + 1) = L + \sum_{l=1}^{L} E_l. \tag{B.16}$$

Finally, performing the change of variable $\xi_i \to z_i = D_i$, we obtain

$$I_{\text{lbl}} = \frac{\mathcal{J}(-i)^L \pi^{\frac{L-n}{2}}}{\prod_{l=1}^{L} \Gamma\left(\frac{D-E_l}{2}\right)} \int_{\mathcal{C}} \frac{\prod_{l=1}^{L} \mathcal{E}_l^{(E_l-D+1)/2} \mathcal{B}_l^{(D-E_l-2)/2}}{z_1^{a_1} \ldots z_n^{a_n}}\, \mathrm{d}^n z. \tag{B.17}$$

In particular, the Jacobian $\mathcal{J}$ can be defined as

$$\mathcal{J} = \frac{1}{\det Y}, \quad \text{where} \quad Y_{ij} = \frac{\mathrm{d}\, z_i}{\mathrm{d}\, \xi_j}. \tag{B.18}$$

For the majority of propagator types, a variable ξ_j of the form k^2 results in a column within Y populated by entries of 0 or ± 1; conversely, selecting ξ_j in the form $k \cdot q$ yields values of 0 or ± 2. Since the system is composed of L variables of the first category and $n - L$ of the second, the fundamental properties of determinants lead us to expect a Jacobian of $\mathcal{J} = \pm 2^{L-n}$.

Thus, the proof is completed by confronting eq. (B.17) with eq. (3.10).

B.3 The Standard Baikov Case

We conclude our computations by deriving the standard Baikov representation, starting from eq. (B.17). In particular, we assume that each individual loop depends on the full set of momenta external to the integral, as well as on all the remaining loop momenta.

In this case, $E_l = E + L - l$ and

$$n = \frac{L(L+1)}{2} + EL. \tag{B.19}$$

Furthermore, by identifying $\mathcal{E}_l = \mathcal{B}_{l+1}$, it follows that the powers to which these polynomials are raised become each other's negatives. Consequently, these terms cancel telescopically in pairs, leaving only $\mathcal{B}_1$ and $\mathcal{E}_L$ as the surviving factors, which we shall redefine as $\mathcal{B}$ and $\mathcal{E}$ for simplicity.

Thus, performing the usual change of variables $\xi_i \to z_i$ we obtain

$$I = \frac{\mathcal{J}(-i)^L \pi^{(L-n)/2} \mathcal{E}^{(\mathcal{E}-d+1)/2}}{\prod_{l=1}^{L} \Gamma\left(\frac{d-\mathcal{E}-L+l}{2}\right)} \int_{\mathcal{C}} \frac{\mathcal{B}(z)^{(d-\mathcal{E}-L-1)/2}}{z_1^{a_1} \dots z_n^{a_n}} \, \mathrm{d}^n z, \tag{B.20}$$

where we have exploited the fact that $\mathcal{E}$ can be factored out of the integral, as it is constructed exclusively from momenta external to the final loop in the integration sequence. Consequently, it possesses no dependence on the loop momenta and, by extension, on the Baikov variables x. By appropriately shifting the indices of the Gamma functions, we recover the standard Baikov representation given in (3.1).

This concludes the formal derivation of both versions of the Baikov representation, proceeding from the initial momentum-space formulation.

C

IBP Reduction with FiniteFlow

In this appendix we review and summarize the technique employed to build a dataflow graph with `FiniteFlow`, following the treatment presented in [17], in order to find the MIs for a given multi-loop integral family. Firstly, a dataflow graph is a directed graph, representing a given numerical computation. It is composed of *nodes*, which represent the numerical algorithm used in the calculation and *arrows*, i.e. the numerical data of fixed length on which the algorithm acts.

Furthermore, in each graph there are two special nodes, namely the *input node*, respresenting only the input numerical values of the graph, and the *output node*, which can be any node chosen to be the output of the program. However, there could be some algorithms whose output length can not be known a priori. For example, if a node solves a linear system, we may not know how many solutions we get. This is the reason why there is another kind of node, the *learning node*, which will be used in our integral reduction program. Specifically, the length of the output of this kind of nodes, can be learned after the *learning phase*, which consists in few numerical evaluations, depending on the algorithm of the node.

As we mentioned in Chapter 4, we can use `FiniteFlow` framework to reduce to the MIs of a given integral family. In practice, finding the MIs is crucial, since they can be used to compute the scattering amplitude of a given process. In fact, consider a generic integral family as in eq. (2.19). We can write a generic amplitude as a linear combination of family integrals I_j

$$A = \sum_{j \in \vec{a}} b_j I_j, \tag{C.1}$$

where the rational coefficients b_j depend only on the kinematics and the dimensional parameter ϵ. Recalling that $\{G_k\} \subset \{I_j\}$, where $\{G_k\}$ is the set of the MIs of the family, we can write

$$I_j = \sum_k c_{jk} G_k. \tag{C.2}$$

As we said before, this derivation is the crucial point of the integral reduction. We can either compute the MIs with Laporta algorithm or building a dataflow graph, whose nodes are able to extract the coefficients

$$A_k = \sum_j b_j c_{jk}, \tag{C.3}$$

so that a generic amplitude can be written as

$$A = \sum_{k \in \text{MIs}} A_k G_k. \tag{C.4}$$

We can sketch the computation with a four-node graph:

- The input node contains a vector $\{\epsilon, \vec{x}\}$, where $\vec{x}$ can be any number of kinematic invariants such as masses or Mandelstam invariants.
- The node b_j computes the rational coefficient in eq. (C.1), taking $\{\epsilon, \vec{x}\}$ as input.
- The coefficients c_{jk} are computed by a sparse linear solver IBP node. Specifically, this node takes $\{\epsilon, \vec{x}\}$ as input and solves numerically the IBP system. This is the core of our program, since we do not know a priori how many MIs we get, this node has a learning phase.
- The output node is a matrix multiplication between the node b_j and the IBP node.

Notice that the MIs appear also in the r.h.s. of eq. (C.1), making the c_{jk} extraction in the IBP node inconsistent. This happens because the IBP node returns a $n_{\text{MIs}} \times n_{\text{non-MIs}}$ matrix, while the a_j node has dimension $n_{\text{MIs}} + n_{\text{non-MIs}}$. We can fix this problem by adding a trivial node which reduces the MIs to themselves. In other words, we add in the graph a no-input node which consists of the identity matrix $\mathbb{I}_{n_{\text{MIs}}}$. Then, if we chain this extra node to the IBP node, we obtain a matrix containing the reduction for all $n_{\text{MIs}} + n_{\text{non-MIs}}$ integrals and the matrix multiplication in the output node is well defined.

Thus, instead of computing large and complex IBP systems, we can build a dataflow graph which avoids the algebraic botteleneck computation and can reconstruct analitically the rational coefficient of the amplitude.

Bibliography

[1] Y. A. Simonov and J. Tjon, "The feynman-schwinger representation for the relativistic two-particle amplitude in field theory", Annals of Physics **228**, 1–18 (1993).

[2] T. Nieuwenhuis and J. Tjon, "Nonperturbative study of generalized ladder graphs in a ϕ 2 χ theory", Physical review letters **77**, 814 (1996).

[3] N. Brambilla and A. Vairo, "From the feynman-schwinger representation to the nonperturbative relativistic bound state interaction", Physical Review D **56**, 1445 (1997).

[4] R. N. Lee and A. A. Pomeransky, "Critical points and number of master integrals", Journal of High Energy Physics **2013**, 10.1007/jhep11(2013)165 (2013).

[5] P. A. Baikov, *Explicit solutions of the n–loop vacuum integral recurrence relations*, 1996.

[6] P. Baikov, "Explicit solutions of the multi-loop integral recurrence relations and its application", Nuclear Instruments and Methods in Physics Research Section A: Accelerators, Spectrometers, Detectors and Associated Equipment **389**, 347–349 (1997).

[7] P. Baikov, "A practical criterion of irreducibility of multi-loop feynman integrals", Physics Letters B **634**, 325–329 (2006).

[8] H. Frellesvig and C. G. Papadopoulos, "Cuts of feynman integrals in baikov representation", Journal of High Energy Physics **2017**, 10.1007/jhep04(2017)083 (2017).

[9] F. V. Tkachov, "A theorem on analytical calculability of 4-loop renormalization group functions", Physics Letters B **100**, 65–68 (1981).

[10] K. G. Chetyrkin and F. V. Tkachov, "Integration by parts: The algorithm to calculate beta-functions in 4 loops", Nuclear Physics B **192**, 159–204 (1981).

[11] K. J. Larsen and Y. Zhang, "Integration-by-parts reductions from unitarity cuts and algebraic geometry", Physical Review D **93**, 10.1103/physrevd.93.041701 (2016).

[12] H. Ita, "Two-loop integrand decomposition into master integrals and surface terms", Physical Review D **94**, 10.1103/physrevd.94.116015 (2016).

[13] Z. Wu, J. Boehm, R. Ma, H. Xu, and Y. Zhang, *Neatibp 1.0, a package generating small-size integration-by-parts relations for feynman integrals*, 2024.

[14] H. Frellesvig, F. Gasparotto, M. K. Mandal, P. Mastrolia, L. Mattiazzi, and S. Mizera, "Vector space of feynman integrals and multivariate intersection numbers", Physical Review Letters **123**, 10.1103/physrevlett.123.201602 (2019).

[15] A. Kotikov, "Differential equations method. new technique for massive feynman diagram calculation", Physics Letters B **254**, 158–164 (1991).

[16] T. Gehrmann and E. Remiddi, "Differential equations for two-loop four-point functions", Nuclear Physics B **580**, 485–518 (2000).

[17] T. Peraro, "Finiteflow: multivariate functional reconstruction using finite fields and dataflow graphs", Journal of High Energy Physics **2019**, 10.1007/jhep07(2019)031 (2019).

[18] Laporta, International Journal of Modern Physics A **15**, 5087 (2000).

[19] S. Badger, J. Henn, J. C. Plefka, and S. Zoia, *Scattering amplitudes in quantum field theory* (Springer International Publishing, 2024).

[20] M. D. Schwartz, *Quantum Field Theory and the Standard Model* (Cambridge University Press, Mar. 2014).

[21] M. E. Peskin and D. V. Schroeder, *An Introduction to quantum field theory* (Addison-Wesley, Reading, USA, 1995).

[22] V. A. Smirnov, *Analytic tools for Feynman integrals*, Vol. 250 (2012).

[23] T. Peraro, *Lecture notes on "Multiloop Techniques"*, 6th School of Analytic Computing in High-Energy and Gravitational Physics, Casa della Cultura, Atrani (Italy), Organized by CERN. Available at: https://indico.cern.ch/event/1244439/, 2023.

[24] X. Guan, X. Liu, Y.-Q. Ma, and W.-H. Wu, *Blade: a package for block-triangular form improved feynman integrals decomposition*, 2025.

[25] C. Anastasiou and A. Lazopoulos, "Automatic integral reduction for higher order perturbative calculations", Journal of High Energy Physics **2004**, 046–046 (2004).

[26] A. Smirnov and F. Chukharev, "Fire6: feynman integral reduction with modular arithmetic", Computer Physics Communications **247**, 106877 (2020).

[27] J. Klappert, F. Lange, P. Maierhöfer, and J. Usovitsch, "Integral reduction with kira 2.0 and finite field methods", Computer Physics Communications **266**, 108024 (2021).

[28] A. von Manteuffel and C. Studerus, *Reduze 2 - distributed feynman integral reduction*, 2012.

[29] A. Georgoudis, K. J. Larsen, and Y. Zhang, "Azurite: an algebraic geometry based package for finding bases of loop integrals", Computer Physics Communications **221**, 203–215 (2017).

[30] J. M. Henn, "Lectures on differential equations for feynman integrals", Journal of Physics A: Mathematical and Theoretical **48**, 153001 (2015).

[31] J. Henn, B. Mistlberger, V. A. Smirnov, and P. Wasser, "Constructing d-log integrands and computing master integrals for three-loop four-particle scattering", Journal of High Energy Physics **2020**, 10.1007/jhep04(2020)167 (2020).

[32] J. M. Henn, "Multiloop integrals in dimensional regularization made simple", Physical Review Letters **110**, 10.1103/physrevlett.110.251601 (2013).

[33] F. Van der Veken, "Wilson lines : applications in QCD", PhD thesis (Antwerp U., Antwerp U., 2014).

[34] A. B. Goncharov, M. Spradlin, C. Vergu, and A. Volovich, "Classical polylogarithms for amplitudes and wilson loops", Physical Review Letters **105**, 10.1103/physrevlett.105.151605 (2010).

[35] C. Anastasiou and K. Melnikov, "Higgs boson production at hadron colliders in nnlo qcd", Nuclear Physics B **646**, 220–256 (2002).

[36] R. E. Cutkosky, "Singularities and discontinuities of Feynman amplitudes", J. Math. Phys. **1**, 429–433 (1960).

[37] C. Vergu, *Cutkosky representation and direct integration*, 2023.

[38] H. Frellesvig, *The loop-by-loop baikov representation – strategies and implementation*, 2025.

[39] R. M. Schabinger, "A new algorithm for the generation of unitarity-compatible integration by parts relations", Journal of High Energy Physics **2012**, 10.1007/jhep01(2012)077 (2012).

[40] S. Weinzierl, *Feynman Integrals. A Comprehensive Treatment for Students and Researchers*, UNITEXT for Physics (Springer, 2022).

[41] A. G. Grozin, "Integration by parts: an introduction", International Journal of Modern Physics A **26**, 2807–2854 (2011).

[42] P. Mastrolia and S. Mizera, "Feynman integrals and intersection theory", Journal of High Energy Physics **2019**, 10.1007/jhep02(2019)139 (2019).

[43] H. Frellesvig, C. Vergu, M. Volk, and M. von Hippel, "Cuts and isogenies", Journal of High Energy Physics **2021**, 10.1007/jhep05(2021)064 (2021).

[44] G. Bertolini, G. Fontana, and T. Peraro, *Calico: computing annihilators from linear identities constraining (differential) operators*, June 2025.

[45] J. Gluza, K. Kajda, and D. A. Kosower, "Towards a basis for planar two-loop integrals", Phys. Rev. D **83**, 045012 (2011).

[46] J. Böhm, A. Georgoudis, K. J. Larsen, M. Schulze, and Y. Zhang, "Complete sets of logarithmic vector fields for integration-by-parts identities of feynman integrals", Physical Review D **98**, 10.1103/physrevd.98.025023 (2018).

[47] V. Chestnov, G. Fontana, and T. Peraro, "Reduction to master integrals and transverse integration identities", Journal of High Energy Physics **2025**, 10.1007/jhep03(2025)113 (2025).

[48] T. Peraro, "Scattering amplitudes over finite fields and multivariate functional reconstruction", Journal of High Energy Physics **2016**, 10.1007/jhep12(2016)030 (2016).

[49] J. Chen, X. Jiang, C. Ma, X. Xu, and L. L. Yang, "Baikov representations, intersection theory, and canonical feynman integrals", Journal of High Energy Physics **2022**, 10.1007/jhep07(2022)066 (2022).

[50] X. Jiang and L. L. Yang, "Recursive structure of baikov representations: generics and application to symbology", Physical Review D **108**, 10.1103/physrevd.108.076004 (2023).

[51] D. Binosi and J. Papavassiliou, "Pinch technique: theory and applications", Physics Reports **479**, 1–152 (2009).

[52] C. Anastasiou, J. Tausk, and M. Tejeda-Yeomans, "The on-shell massless planar double box diagram with an irreducible numerator", Nuclear Physics B - Proceedings Supplements **89**, 262–267 (2000).

[53] M. Zeng, "Differential equations on unitarity cut surfaces", Journal of High Energy Physics **2017**, 10.1007/jhep06(2017)121 (2017).